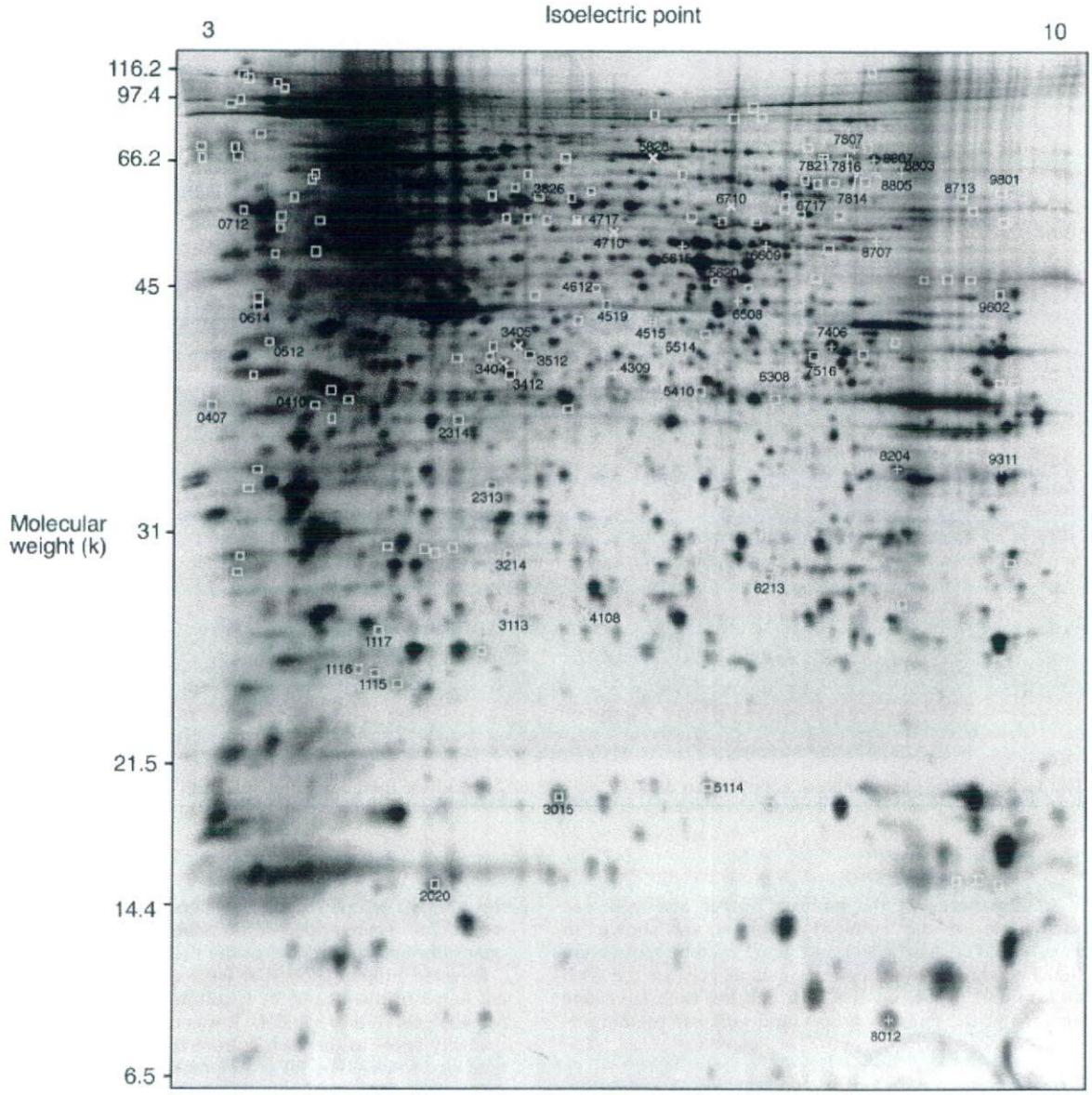

Fig. 2. 2-DE gel of the embryo proper from a cultured rat embryo equivalent to day 11.5. Quantitatively different spots between the 48 and 24 h culture are indicated by a cross (larger in 48 h) or a plus (larger in 24 h) with their SSP. Embryo proper specific spots are indicated by a square and their SSP is shown if its protein was identified.

proteins that were thought to play important roles in developmental process, for example, acidic calponin (SSP 3512), cellular retinoic acid binding protein 2 (SSP 2020), cofilin 1 (SSP 5114), myosin light chain 1 (SSP 1117), and stathmin 1 (SSP 3015) in the embryo proper, and Ash-m (SSP 4214), dimerization cofactor of hepatocyte nuclear factor 1 alpha (SSP 5005), ERM-binding phosphoprotein (SSPs 4303, 4701), prepro-cathepsin L (SSP 0302), and legumain precursor (SSPs 3515, 4503) in the yolk sac membrane. It was noted that multiple spots of complement component 3 (SSPs 1010, 1017, 2108, 2311, 3006, 4105, 4304, 4306, 5111, 8009), which appeared smaller than its intact molecule, were detected only in the yolk sac but not in the embryo proper.

Some proteins were detected in both embryo proper and yolk sac membranes as different protein spots. Adenosine kinase, eukaryotic translation initiation factor 4E, nucleophosmin 1, and protein SET were detected in both embryo proper (SSPs 4612, 3214, 0410, 0512, 0614) and yolk sac membrane (SSPs 4505, 4109, 0004, 4104), but their spots were different (Tables 4–6). Malate dehydrogenase was detected as a soluble form in the embryo

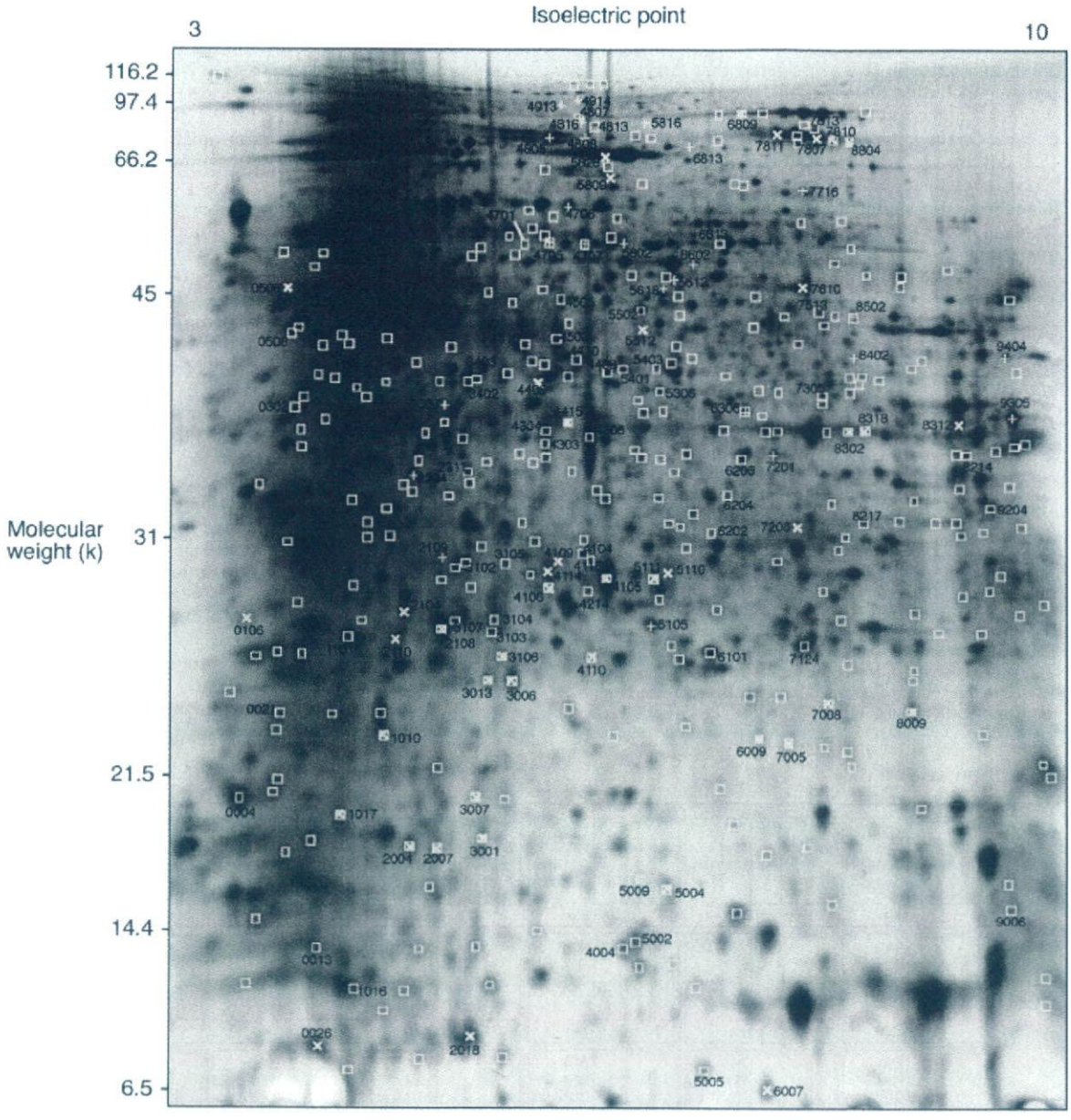

Fig. 3. 2-DE gel of the yolk sac membrane from a cultured rat embryo equivalent to day 11.5. Quantitatively different protein spots between the 48 and 24 h culture are indicated by a cross (larger in 48 h) or a plus (larger in 24 h) with their SSP. Yolk sac membrane specific spots are indicated by a square and their SSP is shown if its protein was identified.

proper (SSP 2314) and as a mitochondrial form in the yolk sac membrane (SSP 8214).

DISCUSSION

The present study showed 2-DE profiles of cultured rat embryos at an early postimplantation stage. When 2-DE profiles of the embryo proper and yolk sac membrane were compared between the 48 and 24 h cultures, there were quantitative but no qualitative differences in the protein spots. It has been shown that specific proteins were observed corresponding to the developmental stages in the postimplantation rodent embryos when analyzed by 2-DE (Greene et al., 2002). It is, therefore, considered that the developmental stage reached by the cultured rat embryos is comparable irrespective of the length of culture period in spite of varied growth as determined by the size of embryos.

Quantitative differences in the protein spots between the 48 and 24 h culture might be related to the varied embryonic growth. It is considered that larger-quantity proteins including RNA-binding proteins in the embryo proper might support better embryonic growth in the 24 h culture. On the other hand, the yolk sac membrane in the 48 h culture seems to have stored an excess amount of serum proteins from the culture medium that should have been digested and supplied as nutrients (Lloyd et al., 1998) to the embryo proper. In the yolk sac membrane, a smaller quantity of constitutive enzymes, relative to the larger quantity in the 24 h culture, may indicate less activity of the yolk sac membrane in the 48 h culture.

Table 2
Summary of Quantitative Differences in 2-DE Profiles of Rat Embryos at day 11.5 by the Varied Length of Culture Period

	Total number of matched spots	Larger quantity in 48 h culture from day 9.5	Larger quantity in 24 h culture from day 10.5
Embryo proper	853	7	18
Yolk sac membrane	1,087	45	26

The number of protein spots whose quantities are significantly different between the 48 and 24 h culture by the t-test ($P<0.01$) is shown. The distribution of the number of larger-quantity spots between the embryo proper and yolk sac membrane is significantly different when analyzed by the Fisher's exact test ($P=0.0015$).

From the protein spots specific to either of the embryo proper or yolk sac membrane, proteins involved in tissue-characteristic functions, such as morphogenesis in the former and nutritional transfer in the latter, could be identified. In the embryo proper, acidic calponin may be involved in brain development (Ferhat et al., 1996). Cellular retinoic acid binding protein 2 has some role in retinoic acid synthesis and retinoid signaling during morphogenesis (Ruberte et al., 1992; Zheng et al., 1999). Cofilin 1 is developmentally regulated, and is required for neural tube morphogenesis and neural crest cell migration (Greene et al., 2002; Gurniak et al., 2005). Myosin light chain 1 is expressed in cardiac development (Lyons et al., 1990). Stathmin 1 may regulate cell proliferation, differentiation, and maturation (Koppel et al., 1990). In the yolk sac membrane, Ash-m may regulate endocytosis for the uptake of nutrients (Miki et al., 1994; Watanabe et al., 1995). Dimerization cofactor of hepatocyte nuclear factor 1 alpha may regulate yolk sac–specific transthyretin expression (Cereghini et al., 1992; Costa et al., 1990). ERM-binding phosphoprotein might be involved in receptor recycling in endocytosis (Brent et al., 1990; Li et al., 2002). Cathepsin L (Sol-Church et al., 1999) and legumain (Ambroso and Harris, 1994; Shirahama-Noda et al., 2003) are lysosomal proteases important for histiotrophic nutrition.

Multiple spots of complement component 3 (C3) in the yolk sac membrane are considered to be the digestive

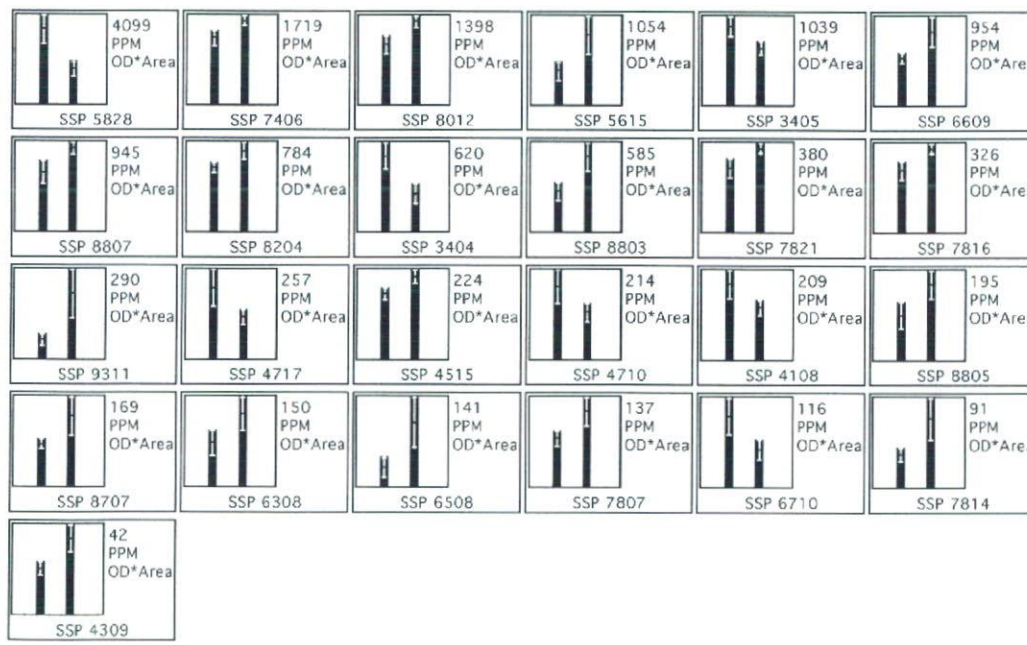

Fig. 4. Quantity of protein spots with significant differences between the 48 and 24 h culture in the embryo proper. Mean and SD ranges are shown in the bars (left for 48 h and right for 24 h) in the boxes for individual protein spots as indicated by SSP. The boxes are arranged from the top left to the right in the descending order of the spot quantity in the 48 h culture. Mean quantity of the larger-quantity spots between the 48 and 24 h culture are indicated as ppm of the total density in the gel image at the top right in each box.

Fig. 5. Quantity of protein spots with significant differences between the 48 and 24 h culture in the yolk sac membrane. Mean and SD ranges are shown in the bars (left for 48 h and right for 24 h) in the boxes for individual protein spots as indicated by SSP. The boxes are arranged from the top left to the right in the descending order of the spot quantity in the 48 h culture. Mean quantity of the larger-quantity spots between the 48 and 24 h culture are indicated as ppm of the total density in the gel image at the top right in each box.

Table 3
Identified Protein Spots With Quantitative Differences Between the 24 and 48 h Culture in the Embryo Proper

SSP	Protein name	Nominal mass	Calculated pI	Accession No.
Larger quantity in 48 h culture				
4108	DJ-1 protein [Rattus norvegicus]	20190	6.32	gi|16924002
5828	Albumin [Rattus norvegicus]	70670	6.09	gi|19705431
Larger quantity in 24 h culture				
4515	Poly(rC) binding protein 2 [Rattus norvegicus]	38955	6.33	gi|61557337
	AND			
	TAR DNA binding protein isoform 1 [Mus musculus]	44918	6.36	gi|21704096
5615	Mitochondrial aldehyde dehydrogenase precursor [Rattus norvegicus]	56079	6.69	gi|45737866
7406	PREDICTED: similar to Poly(rC)-binding protein 1 (Alpha-CP1)(hnRNP-E1) [Rattus norvegicus]	37987	6.66	gi|6754994
7807	Transferrin [Rattus norvegicus]	78512	7.14	gi|61556986
7821	Far upstream element (FUSE) binding protein 1 [Rattus norvegicus]	67326	7.18	gi|83320094
8012	Macrophage migration inhibitory factor	12709	7.74	gi|694108
8204	B-36 VDAC = 36 kda voltage dependent anion channel [rats, hippocampus, Peptide, 295 aa]	32327	7.44	gi|299036
8803	Transketolase [Rattus norvegicus]	71940	7.54	gi|12018252
8807	Far upstream element (FUSE) binding protein 1 [Rattus norvegicus]	67326	7.18	gi|83320094

Table 4
Identified Protein Spots With Quantitative Differences Between the 24 and 48 h Culture in the Yolk Sac Membrane

SSP	Protein name	Nominal mass	Calculated pI	Accession No.
Larger quantity in 48 h culture				
0026	Tubulin, alpha 1 [Rattus norvegicus]	50816	4.94	gi|38328248
	OR			
	Tubulin, alpha 6 [Rattus norvegicus]	50590	4.96	gi|58865558
0106	Membrane-associated progesterone receptor component 1 (Acidic 25-kDa protein) (25-DX)	21699	4.45	gi|6647578
0506	Reticulocalbin 3, EF-hand calcium binding domain [Rattus norvegicus]	37918	4.72	gi|56744249
1010	PREDICTED: similar to Programmed cell death protein 6 (Probable calcium-binding protein ALG-2) (PMP41) (ALG-257) [Rattus norvegicus]	21948	5.36	gi|34853323
	AND			
	Alpha-1-macroglobulin	168388	6.46	gi|202857
	OR			
	Pregnancy-zone protein [Rattus norvegicus]	168422	6.46	gi|21955142
	AND			
	Complement component 3 [Rattus norvegicus]	187825	6.12	gi|8393024
1017	Complement component 3 [Rattus norvegicus]	187825	6.12	gi|8393024
2018	Complement component 3 [Rattus norvegicus]	187825	6.12	gi|8393024
2108	Complement component 3 [Rattus norvegicus]	187825	6.12	gi|8393024
3001	Actin related protein 2/3 complex, subunit 5 [Rattus norvegicus]	16367	5.47	gi|71043638
3006	Complement component 3 [Rattus norvegicus]	187825	6.12	gi|8393024
4105	Complement component 3 [Rattus norvegicus]	187825	6.12	gi|8393024
4109	Eukaryotic translation initiation factor 4E [Rattus norvegicus]	25266	5.79	gi|16758870
4415	Serine (or cysteine) peptidase inhibitor, clade F, member 2 [Rattus norvegicus]	55086	5.74	gi|58865362
5111	Complement component 3 [Rattus norvegicus]	187825	6.12	gi|8393024
	AND			
	Heat shock 90-kDa protein 1, beta [Rattus norvegicus]	83631	4.97	gi|51859516
5828	Albumin [Rattus norvegicus]	70670	6.09	gi|19705431
7807	Transferrin [Rattus norvegicus]	78512	7.14	gi|61556986
8009	Complement component 3 [Rattus norvegicus]	187825	6.12	gi|8393024

Table 4
Continued

SSP	Protein name	Nominal mass	Calculated pI	Accession No.
8302	Glyceraldehyde-3-phosphate dehydrogenase [Rattus norvegicus]	36090	8.14	gi|8393418
	AND			
	Aldolase A	39691	8.31	gi|202837
Larger quantity in 24 h culture				
4706	Protein disulfide-isomerase A3 precursor (Disulfide isomerase ER-60) (ERp60) (58 kDa microsomal protein) (p58) (ERp57) (HIP-70) (Q-2)	57044	5.88	gi|1352384
4707	Liver annexin-like protein [Rattus norvegicus]	52036	5.99	gi|7108713
	OR			
	Plasma glutamate carboxypeptidase [Rattus norvegicus]	51994	6.09	gi|13928880
	OR			
	Pgcp protein [Rattus norvegicus]	52066	5.99	gi|47477878
5602	Liver annexin-like protein [Rattus norvegicus]	52036	5.99	gi|7108713
5618	PREDICTED: similar to adenylosuccinate synthetase, non muscle [Rattus norvegicus]	50453	5.98	gi|34880967
6602	Enolase 1, alpha [Rattus norvegicus]	47428	6.16	gi|6978809
7201	PREDICTED: similar to Glucosamine-6-phosphate isomerase (Glucosamine-6-phosphate deaminase) (GNPDA) (GlcN6P deaminase) (Oscillin) [Rattus norvegicus]	32730	6.27	gi|109507234
8502	Arginosuccinate synthetase [Rattus norvegicus]	46752	7.63	gi|25453414
9404	Peroxisomal 3-ketoacyl-CoA thiolase A [Rattus norvegicus]	45324	8.53	gi|220849

Table 5
Identified Protein Spots Specific to the Embryo Proper of Cultured Rat Embryos

SSP	Protein name	Nominal mass	Calculated pI	Accession No.
0407	Methylosome subunit pICln (Chloride conductance regulatory protein ICln) (I(Cln)) (Chloride channel, nucleotide sensitive 1A)	26190	3.97	gi|544031
0410	Nucleophosmin 1 [Rattus norvegicus]	32711	4.62	gi|7242160
0512	Protein SET (Phosphatase 2A inhibitor I2PP2A) (I-2PP2A) (Template-activating factor I) (TAF-I) (Liver regeneration-related protein LRRGR00002)	33386	4.22	gi|46396568
0614	Protein SET (Phosphatase 2A inhibitor I2PP2A) (I-2PP2A) (Template-activating factor I) (TAF-I) (Liver regeneration-related protein LRRGR00002)	33386	4.22	gi|46396568
0712	Nucleosome assembly protein 1-like 1 [Rattus norvegicus]	45630	4.36	gi|77404363
1115	PREDICTED: similar to Chromobox protein homolog 5 (Heterochromatin protein 1 homolog alpha) (HP1 alpha) [Rattus norvegicus].	22343	5.71	gi|27665448
1116	Chromobox homolog 3 [Rattus norvegicus].	20969	5.23	gi|15082258
1117	Myosin light polypeptide 4 (Myosin light chain 1, atrial isoform)	21383	4.96	gi|127140
2020	Cellular retinoic acid binding protein 2 [Rattus norvegicus]	16094	5.23	gi|25453404
2313	p32-Subunit of replication protein A [Rattus norvegicus]	28980	5.47	gi|1403534
2314	Malate dehydrogenase 1, NAD (soluble) [Rattus norvegicus]	36631	6.16	gi|15100179
	OR			
	Lactate dehydrogenase A [Rattus norvegicus]	36712	8.45	gi|8393706
	AND			
	Dermal papilla derived protein 6 [Rattus norvegicus]	35810	5.15	gi|48843729
3015	Stathmin 1 [Rattus norvegicus]	17278	5.76	gi|8393696
3113	RAB11B, member RAS oncogene family [Rattus norvegicus]	24588	5.64	gi|14249144
3214	Eukaryotic translation initiation factor 4E [Rattus norvegicus]	25266	5.79	gi|16758870
3412	PREDICTED: similar to Eukaryotic translation initiation factor 3 subunit 2 (eIF-3 beta) (eIF3 p36) (eIF3i) (TGF-beta receptor-interacting protein 1) (TRIP-1) [Rattus norvegicus]	36837	5.38	gi|109477318
3512	Calponin 3, acidic [Rattus norvegicus]	36583	5.47	gi|9506501
3826	Serine/threonine-protein kinase PAK 2 (p21-activated kinase 2) (PAK-2) (Gamma-PAK) (p62-PAK)	58209	5.57	gi|2499648
	AND			
	Myo-inositol 1-phosphate synthase A1 [Rattus norvegicus]	48551	5.67	gi|62078495

Table 5
Continued

SSP	Protein name	Nominal mass	Calculated pI	Accession No.
4515	Poly(rC) binding protein 2 [Rattus norvegicus]	38955	6.33	gi|61557337
	AND			
	TAR DNA binding protein isoform 1 [Mus musculus]	44918	6.36	gi|21704096
4519	PREDICTED: similar to protein phosphatase methylesterase 1 [Rattus norvegicus]	42688	5.67	gi|62641013
4612	Adenosine kinase [Rattus norvegicus]	40415	5.84	gi|1906013
	AND			
	2-Oxoisovalerate dehydrogenase subunit alpha, mitochondrial precursor (Branched-chain alpha-keto acid dehydrogenase E1 component alpha chain) (BCKDH E1-alpha)	50418	7.68	gi|129032
5114	Cofilin 1 [Rattus norvegicus]	18749	8.22	gi|8393101
5410	Protein phosphatase 1, catalytic subunit, gamma isoform [Rattus norvegicus]	37701	6.12	gi|11968062
	AND			
	mRNA decapping enzyme [Rattus norvegicus]	38804	6.02	gi|23463287
	AND			
	PRP4 protein kinase homolog [Mus musculus]	96187	10.45	gi|3236351
5514	PREDICTED: similar to RIKEN cDNA 1110064P04 [Rattus norvegicus]	45347	7.63	gi|109500109
5620	PREDICTED: similar to DEAD (Asp-Glu-Ala-Asp) box polypeptide 48 [Rattus norvegicus]	47096	6.3	gi|109492318
	AND			
	C-Terminal binding protein 1 [Rattus norvegicus]	47055	6.17	gi|15011859
6213	Hypothetical protein LOC302247 [Rattus norvegicus]	33918	8.73	gi|114145722
6717	Nucleoporin 54kDa [Rattus norvegicus]	55825	6.53	gi|8393855
7516	Arginase-1 (Type I arginase) (Liver-type arginase)	35122	6.76	gi|114146
	AND			
	PREDICTED: similar to peptidylprolyl isomerase D [Rattus norvegicus]	41084	6.48	gi|62655561
7821	Far upstream element (FUSE) binding protein 1 [Rattus norvegicus]	67326	7.18	gi|83320094
8713	Far upstream element (FUSE) binding protein 3 [Rattus norvegicus]	61657	8.45	gi|86129564
9602	Serine (or cysteine) proteinase inhibitor, clade H, member 1 [Rattus norvegicus]	46602	8.88	gi|8393057
9801	Far upstream element (FUSE) binding protein 3 [Rattus norvegicus]	61657	8.45	gi|86129564

fragments from C3 in the culture medium since rat serum used as a culture medium contains a high concentration of C3 (>2 mg/ml) and C3 production in the yolk sac membrane is not known (Colten, 1994; Guiguet et al., 1987). Possibly, each of the multiple spots might have different biological functions because it is known that fragments of C3 function as various effectors. For example, C3b fragment enhances phagocytic activity in mouse placental trophoblasts probably through the CR1 receptor (Albieri et al., 1999; Amarante-Paffaro et al., 2004), and iC3b fragment functions as an embryotrophic factor probably through the Crry and CR3 receptor in mouse blastocysts (Lee et al., 2004).

Different spots of the same proteins between the embryo proper and yolk sac membrane may indicate the presence of isoforms or posttranslational modification of the proteins. There are at least two isoforms of adenosine kinase with tissue-dependent expression in rats (Sakowicz et al., 2001). Eukaryotic translation initiation factor 4E is phosphorylated and cleaved upon apoptosis (Scheper and Proud, 2002). The nucleophosmin spot in the yolk sac membrane may be due to proteolytic degradation that can be influenced by exogenous stimulation (Zhang et al., 2006). Three protein SET spots (two in the embryo proper and one in the yolk sac membrane) could be assigned to three kinds of transcript although their differential expression is not known (Fukukawa et al., 2000). Both soluble and mitochondrial forms of malate dehydrogenase are developmentally regulated and show tissue-specific expression (Greene et al., 2002; Kelly et al., 1989; Lo et al., 2005).

The protein identification data in the present study is consistent with those in our previous study (Usami et al., 2007) and added many identified spots to the 2-DE map of cultured postimplantation rat embryos. Protein spots analyzed in common in the embryo proper between these studies were identified as the same proteins, respectively, verifying the reproducibility of this method; for example, albumin (SSP 5828 and Spot No. 2 in the previous study), hnRNP-E1 (SSP 7406 and Spot No. 81), and stathmin 1 (SSP 3015 and Spot No. 29). From the updated 2-DE map, cofilin 1 (SSP 5114) is considered to be a charge variant probably due to phosphorylation because of its acidic pI sifted from that of previously identified cofilin 1 (Spot No. 25) (Usami et al., 2007) and known functional regulation of cofilin 1 (Sumi et al., 2001). Thus, the 2-DE map is useful across proteomic studies on cultured postimplantation rat embryos.

In conclusion, comparative proteome analysis of the embryo proper and yolk sac membrane of day 11.5 cultured rat embryos by 2-DE showed protein spots specific to each of them that can be related their

Table 6
Identified Protein Spots Specific to the Yolk Sac Membrane of Cultured Rat Embryos

SSP	Protein name	Nominal mass	Calculated pI	Accession No
0004	Nucleophosmin 1 [Rattus norvegicus]	32711	4.62	gi|38014709
0013	PREDICTED: hypothetical protein XP_579384 [Rattus norvegicus]	187746	6.06	gi|62718645
0021	Nucleolin [Rattus norvegicus]	77158	4.67	gi|6981248
0302	PREDICTED: tumor rejection antigen gp96 (predicted) [Rattus norvegicus]	92998	4.72	gi|62651904
	AND			
	Prepro-cathepsin L [Rattus norvegicus]	38232	6.73	gi|55888
0508	Heat shock 90kDa protein 1, beta [Rattus norvegicus]	83631	4.97	gi|51859516
1010	PREDICTED: similar to programmed cell death protein 6 (Probable calcium-binding protein ALG-2) (PMP41) (ALG-257) [Rattus norvegicus]	21948	5.36	gi|34853323
	AND			
	Alpha-1-macroglobulin	168388	6.46	gi|202857
	OR			
	Pregnancy-zone protein [Rattus norvegicus]	168422	6.46	gi|21955142
	AND			
	Complement component 3 [Rattus norvegicus]	187825	6.12	gi|8393024
1016	PREDICTED: similar to germinal histone H4 gene [Rattus norvegicus]	18394	10.93	gi|62648434
	OR			
	PREDICTED: similar to Histone H2B 291B [Rattus norvegicus]	37149	10.56	gi|62663604
1017	Complement component 3 [Rattus norvegicus]	187825	6.12	gi|8393024
1101	Chain A, Catechol O-Methyltransferase	24960	5.11	gi|1633081
	AND			
	Proteasome endopeptidase complex (EC 3.4.25.1) delta chain - rat	21864	4.98	gi|285140
2108	Complement component 3 [Rattus norvegicus]	187825	6.12	gi|8393024
2311	3-Hydroxyanthranilate 3,4-dioxygenase [Rattus norvegicus]	32846	5.57	gi|9910256
	AND			
	Complement component 3 [Rattus norvegicus]	187825	6.12	gi|8393024
3001	Actin related protein 2/3 complex, subunit 5 [Rattus norvegicus]	16367	5.47	gi|71043638
3006	Complement component 3 [Rattus norvegicus]	187825	6.12	gi|8393024
3102	Phosphoserine phosphatase [Rattus norvegicus]	25180	5.49	gi|57527332
3103	Apolipoprotein A-I [Rattus norvegicus]	30100	5.52	gi|6978515
3104	Apolipoprotein A-I [Rattus norvegicus]	30100	5.52	gi|6978515
3105	Phosphoserine phosphatase [Rattus norvegicus]	25180	5.49	gi|57527332
3107	Apolipoprotein A-I [Rattus norvegicus]	30100	5.52	gi|6978515
3402	PREDICTED: similar to Tubulin alpha-2 chain (Alpha-tubulin 2) [Rattus norvegicus]	50932	4.94	gi|62653035
	AND			
	Actin beta - rat	42066	5.29	gi|71620
3403	Eukaryotic translation initiation factor 3, subunit 2 (beta) [Mus musculus]	36837	5.38	gi|9055370
3515	Legumain precursor (Asparaginyl endopeptidase) (Protease, cysteine 1)	49834	6.09	gi|22001735
4004	Expressed in non-metastatic cells 2 [Rattus norvegicus]	17386	6.92	gi|55926145
4104	Protein SET (Phosphatase 2A inhibitor I2PP2A) (I-2PP2A) (Template-activating factor I) (TAF-I) (Liver regeneration-related protein LRRGR00002)	33386	4.22	gi|46396568
4105	Complement component 3 [Rattus norvegicus]	187825	6.12	gi|8393024
4115	Chaperonin subunit 6a (zeta) [Rattus norvegicus]	58437	6.63	gi|76253725
4214	Ash-m [Rattus norvegicus]	23655	6.31	gi|914957
4303	ERM-binding phosphoprotein [Rattus norvegicus]	39149	5.7	gi|11024674
4304	Complement component 3 [Rattus norvegicus]	187825	6.12	gi|8393024
4306	Complement component 3 [Rattus norvegicus]	187825	6.12	gi|8393024
4408	Eukaryotic translation elongation factor 2 [Rattus norvegicus]	96192	6.41	gi|8393296
4410	Elongation factor 2	38690	5.69	gi|203997
4415	Serine (or cysteine) peptidase inhibitor, clade F, member 2 [Rattus norvegicus]	55086	5.74	gi|58865362
4503	Legumain precursor (Asparaginyl endopeptidase) (Protease, cysteine 1)	49834	6.09	gi|22001735
4505	Adenosine kinase [Rattus norvegicus]	40415	5.84	gi|1906013
4701	ERM-binding phosphoprotein [Rattus norvegicus]	39149	5.7	gi|11024674

Table 6
Continued

SSP	Protein name	Nominal mass	Calculated pI	Accession No
4707	Liver annexin-like protein [Rattus norvegicus] OR	52036	5.99	gi|7108713
	Plasma glutamate carboxypeptidase [Rattus norvegicus] OR	51994	6.09	gi|13928880
	Pgcp protein [Rattus norvegicus]	52066	5.99	gi|47477878
4813	Fatty acid synthase	275117	5.96	gi|204099
5002	Transthyretin precursor (Prealbumin) (TBPA)	15824	5.77	gi|136467
5005	Chain A, crystal structure of a complex between the dimerization domain of Hnf-1 alpha and the coactivator Dcoh	11989	6.06	gi|10835702
5111	Complement component 3 [Rattus norvegicus] AND	187825	6.12	gi|8393024
	Heat shock 90-kDa protein 1, beta [Rattus norvegicus]	83631	4.97	gi|51859516
5306	M2 pyruvate kinase [Rattus norvegicus]	58314	7.15	gi|206205
5401	Elongation factor 2	38690	5.69	gi|203997
5403	Gale protein [Rattus norvegicus]	38671	6.02	gi|67678395
5502	Enolase 1, alpha [Rattus norvegicus]	47428	6.16	gi|6978809
6101	Chain A, Crystal Structure Of A Mammalian 2-Cys Peroxiredoxin, Hbp23.	22250	8.34	gi|6435547
6202	Similar to RIKEN cDNA 2810409H07 [Rattus norvegicus]	44792	7.62	gi|76677911
6204	Eukaryotic translation initiation factor 4A, isoform 1 [Rattus norvegicus]	46353	5.32	gi|40786436
6206	Elongation factor 2	38690	5.69	gi|203997
6613	PREDICTED: similar to aldehyde dehydrogenase family 7, member A1 [Rattus norvegicus]	59225	7.99	gi|62664437
7124	H(+)-transporting ATP synthase [Rattus norvegicus] AND	25639	7.03	gi|57029
	Chain A, crystal structure of a mammalian 2-Cys peroxiredoxin, Hbp23.	22250	8.34	gi|6435547
7305	Citrate synthase [Rattus norvegicus]	52176	8.53	gi|18543177
7513	Eukaryotic translation elongation factor 2 [Rattus norvegicus]	96192	6.43	gi|8393296
7813	Serotransferrin precursor (Transferrin) (Siderophilin) (Beta-1-metal-binding globulin) OR	78538	6.94	gi|6175089
	Ab2-417 [Rattus norvegicus]	109510	8.35	gi|33086606
8009	Complement component 3 [Rattus norvegicus]	187825	6.12	gi|8393024
8214	Malate dehydrogenase, mitochondrial [Rattus norvegicus]	36117	8.93	gi|42476181
8217	Adenylate kinase 2 isoform a [Rattus norvegicus] OR	26648	6.33	gi|13591872
	Adenylate kinase 2 isoform b [Rattus norvegicus]	25741	7.01	gi|77020256
8302	Glyceraldehyde-3-phosphate dehydrogenase [Rattus norvegicus] AND	36090	8.14	gi|8393418
	Aldolase A	39691	8.31	gi|202837
8502	Arginosuccinate synthetase [Rattus norvegicus]	46752	7.63	gi|25453414
9006	Eukaryotic translation elongation factor 1 alpha 1 [Rattus norvegicus]	50424	9.1	gi|28460696
9204	Transaminase, Glu oxaloacetic	44678	8.52	gi|350611

characteristic functions. 2-DE profiles of cultured postimplantation rat embryos are considered quantitatively variable according to the culture conditions but qualitatively comparable. Proteomic analysis of cultured postimplantation rat embryos will be a new approach in developmental biology and toxicology at the protein level.

ACKNOWLEDGMENTS

This work was partially supported by the Ministry of Education, Science, Sports and Culture, Grant-in-Aid for Exploratory Research, 15658090, 2003–2005.

REFERENCES

Albieri A, Kipnis T, Bevilacqua E. 1999. A possible role for activated complement component 3 in phagocytic activity exhibited by the mouse trophoblast. Am J Reprod Immunol 41:343–352.

Amarante-Paffaro A, Queiroz GS, Corrêa ST, Spira B, Bevilacqua E. 2004. Phagocytosis as a potential mechanism for microbial defense of mouse placental trophoblast cells. Reproduction 128:207–218.

Ambroso JL, Harris C. 1994. In vitro embryotoxicity of the cysteine proteinase inhibitors benzyloxycarbonyl-phenylalanine-alanine-diazomethane (Z-Phe-Ala-CHN2) and Benzyloxycarbonyl-phenylalanine-phenylalanine-diazomethane (Z-Phe-Phe-CHN2). Teratology 50:214–288.

Brent RL, Beckman DA, Jensen M, Koszalka TR. 1990. Experimental yolk sac dysfunction as a model for studying nutritional disturbances in the embryo during early organogenesis. Teratology 41: 405–413.

Calegari F, Haubensak W, Yang D, Huttner WB, Buchholz F. 2002. Tissue-specific RNA interference in postimplantation mouse embryos with endoribonuclease-prepared short interfering RNA. Proc Natl Acad Sci USA 99:14236–14240.

Cereghini S, Ott MO, Power S, Maury M. 1992. Expression patterns of vHNF1 and HNF1 homeoproteins in early postimplantation embryos suggest distinct and sequential developmental roles. Development 116:783–797.

Colten HR. 1994. Extrahepatic complement gene expression. In: Erdei A, editor. New aspects of complement structure and function. Georgetown, TX: R.G. Landes Company. p 1–13.

Costa RH, Van Dyke TA, Yan C, Kuo F, Darnell JE Jr. 1990. Similarities in transthyretin gene expression and differences in transcription factors: liver and yolk sac compared to choroid plexus. Proc Natl Acad Sci USA 87:6589–6593.

Ferhat L, Charton G, Represa A, Ben-Ari Y, der Terrossian E, Khrestchatisky M. 1996. Acidic calponin cloned from neural cells is differentially expressed during rat brain development. Eur J Neurosci 8:1501–1509.

Fukukawa C, Shima H, Tanuma N, Ogawa K, Kikuchi K. 2000. Up-regulation of I-2(PP2A)/SET gene expression in rat primary hepatomas and regenerating livers. Cancer Lett 161:89–95.

Greene NDE, Leung K-Y, Wait R, Begum S, Dunn MJ, Copp AJ. 2002. Differential protein expression at the stage of neural tube closure in the mouse embryo. J Biol Chem 277:41645–41651.

Guiguet M, Dethieux M-C, Exilie-Frigére M-F, Bidan Y, Lautissier J-L, Mack G. 1987. Third component of rat complement. Purification from plasma and radioimmunoassay in culture media from cell lines. J Immun Methods 96:157–164.

Gurniak CB, Perlas E, Witke W. 2005. The actin depolymerizing factor n-cofilin is essential for neural tube morphogenesis and neural crest cell migration. Dev Biol 278:231–241.

Kelly DP, Gordon JI, Alpers R, Strauss AW. 1989. The tissue-specific expression and developmental regulation of two nuclear genes encoding rat mitochondrial proteins. Medium chain acyl-CoA dehydrogenase and mitochondrial malate dehydrogenase. J Biol Chem 264:18921–18925.

Koppel J, Boutterin MC, Doye V, Peyro-Saint-Paul H, Sobel A. 1990. Developmental tissue expression and phylogenetic conservation of stathmin, a phosphoprotein associated with cell regulations. J Biol Chem 265:3703–3707.

Lee Y-L, Lee K-F, Xu J-S, He Q-Y, Chiu J-F, Lee WM, Luk JM, Yeung WSB. 2004. The embryotrophic activity of oviductal cell-derived complement C3b and iC3b, a novel function of complement protein in reproduction. J Biol Chem 279:12763–12768.

Li JG, Chen C, Liu-Chen LY. 2002. Ezrin-radixin-moesin-binding phosphoprotein-50/Na+/H+ exchanger regulatory factor (EBP50/NHERF) blocks U50,488H-induced down-regulation of the human kappa opioid receptor by enhancing its recycling rate. J Biol Chem 277:27545–27552.

Lloyd JB, Beckman DA, Brent RL. 1998. Nutritional role of the visceral yolk sac in organogenesis-stage rat embryos. Reprod Toxicol 12:193–195.

Lo AS, Liew CT, Ngai SM, Tsui SK, Fung KP, Lee CY, Waye MM. 2005. Developmental regulation and cellular distribution of human cytosolic malate dehydrogenase (MDH1). J Cell Biochem 94:763–773.

Lyons GE, Schiaffino S, Sassoon D, Barton P, Buckingham M. 1990. Developmental regulation of myosin gene expression in mouse cardiac muscle. J Cell Biol 111:2427–2436.

Miki H, Miura K, Matuoka K, Nakata T, Hirokawa N, Orita S, Kaibuchi K, Takai Y, Takenawa T. 1994. Association of Ash/Grb-2 with dynamin through the Src homology 3 domain. J Biol Chem 269: 5489–5492.

Morriss-Kay GM. 1993. Postimplantation mammalian embryos. In: Stern CD, Holland PWH, editors. Essential developmental biology, 1st ed. Oxford: IRL Press. p 55–66.

Potts LF, Sadler TW. 1997. The use of antisense oligonucleotide technology and mouse whole-embryo culture to study gene function during organogenesis. In: Daston GP, editor. Molecular and cellular methods in developmental toxicology. Boca Raton: CRC Press. p 69–92.

Ruberte E, Friederich V, Morriss-Kay G, Chambon P. 1992. Differential distribution patterns of CRABP I and CRABP II transcripts during mouse embryogenesis. Development 115:973–987.

Sakowicz M, Grden M, Pawelczyk T. 2001. Expression level of adenosine kinase in rat tissues. Lack of phosphate effect on the enzyme activity. Acta Biochim Pol 48:745–754.

Scheper GC, Proud CG. 2002. Does phosphorylation of the cap-binding protein eIF4E play a role in translation initiation? Eur J Biochem 269:5350–5359.

Shevchenko A, Wilm M, Vorm O, Mann M. 1996. Mass spectrometric sequencing of proteins from silver-stained polyacrylamide gels. Anal Chem 68:850–858.

Shirahama-Noda K, Yamamoto A, Sugihara K, Hashimoto N, Asano M, Nishimura M, Hara-Nishimura I. 2003. Biosynthetic processing of cathepsins and lysosomal degradation are abolished in asparaginyl endopeptidase-deficient mice. J Biol Chem 278:33194–33199.

Sol-Church K, Shipley J, Beckman DA, Mason R. 1999. Expression of cysteine proteases in extraembryonic tissues during mouse embryogenesis. Arch Biochem Biophys 372:375–381.

Sumi T, Matsumoto K, Nakamura T. 2001. Specific activation of LIM kinase 2 via phosphorylation of threonine 505 by ROCK, a Rho-dependent protein kinase. J Biol Chem 276:670–676.

Usami M, Ohno Y. 1996. Teratogenic effects of selenium compounds on cultured postimplantation rat embryos. Teratog Carcinog Mutagen 16:27–36.

Usami M, Mitsunaga K, Nakazawa K. 2007. Two-dimensional electrophoresis of protein from cultured postimplantation rat embryos for developmental toxicity studies. Toxicol In Vitro 21:521–526.

Van Maele-Fabry G, Clotman F, Gofflot F, Bosschaert J, Picard JJ. 1997. Postimplantation mouse embryos cultured in vitro. Assessment with whole-mount immunostaining and in situ hybridization. Int J Dev Biol 41:365–374.

Watanabe K, Fukuchi T, Hosoya H, Shirasawa T, Matuoka K, Miki H, Takenawa T. 1995. Splicing isoforms of rat Ash/Grb2. Isolation and characterization of the cDNA and genomic DNA clones and implications for the physiological roles of the isoforms. J Biol Chem 270:13733–13739.

Williams JA, Mann FM, Brown NA. 1997. Gene expression domains as markers in developmental toxicity studies using mammalian embryo culture. Int J Dev Biol 41:359–364.

Zhang X, Kuramitsu Y, Fujimoto M, Hayashi E, Yuan X, Nakamura K. 2006. Proteomic analysis of macrophages stimulated by lipopolysaccharide: Lipopolysaccharide inhibits the cleavage of nucleophosmin. Electrophoresis 27:1659–1668.

Zheng WL, Bucco RA, Sierra-Rievera E, Osteen KG, Melner MH, Ong DE. 1999. Synthesis of retinoic acid by rat ovarian cells that express cellular retinoic acid-binding protein-II. Biol Reprod 60:110–114.

THE JOURNAL OF BIOLOGICAL CHEMISTRY VOL. 282, NO. 35, pp. 25659–25667, August 31, 2007

Essential, Completely Conserved Glycine Residue in the Domain III S2–S3 Linker of Voltage-gated Calcium Channel α_1 Subunits in Yeast and Mammals*[S]

Received for publication, May 7, 2007 Published, JBC Papers in Press, June 14, 2007, DOI 10.1074/jbc.M703757200

Kazuko Iida[‡1], Jinfeng Teng[§¶1], Tomoko Tada[§¶2], Ayaka Saka[§3], Masumi Tamai[§], Hiroko Izumi-Nakaseko[‖], Satomi Adachi-Akahane[‖], and Hidetoshi Iida[§¶4]

From the [‡]Biomembrane Signaling Project 2, Tokyo Metropolitan Institute of Medical Science, 3-18-22 Honkomagome, Bunkyo-ku, Tokyo 113-8613, the [§]Department of Biology, Tokyo Gakugei University, 4-1-1 Nukui kita-machi, Koganei-shi, Tokyo 184-8501, the [¶]CREST, Japan Science and Technology Agency, 4-1-8 Honcho, Kawaguchi-shi, Saitama 332-0012, and the [‖]Department of Pharmacology, School of Medicine, Faculty of Medicine, Toho University, 5-21-16 Omori-Nishi, Ota-ku, Tokyo 143-8540, Japan

Voltage-gated Ca^{2+} channels (VGCCs) mediate the influx of Ca^{2+} that regulates many cellular events, and mutations in VGCC genes cause serious hereditary diseases in mammals. The yeast *Saccharomyces cerevisiae* has only one gene encoding the putative pore-forming α_1 subunit of VGCC, *CCH1*. Here, we identify a *cch1* allele producing a completely nonfunctional Cch1 protein with a Gly^{1265} to Glu substitution present in the domain III S2–S3 cytoplasmic linker. Comparison of amino acid sequences of this linker among 58 VGCC α_1 subunits from 17 species reveals that a Gly residue whose position corresponds to that of the Cch1 Gly^{1265} is completely conserved from yeasts to humans. Systematic amino acid substitution analysis using 10 amino acids with different chemical and structural properties indicates that the Gly^{1265} is essential for Cch1 function because of the smallest residue volume. Replacement of the Gly^{959} residue of a rat brain $Ca_v1.2$ α_1 subunit (rbCII), positionally corresponding to the yeast Cch1 Gly^{1265}, with Glu, Ser, Lys, or Ala results in the loss of Ba^{2+} currents, as revealed by the patch clamp method. These results suggest that the Gly residue in the domain III S2–S3 linker is functionally indispensable from yeasts to mammals. Because the Gly residue has never been studied in any VGCC, these findings provide new insights into the structure-function relationships of VGCCs.

Voltage-gated Ca^{2+} channels (VGCCs)[5] in the plasma membrane mediate the influx of Ca^{2+} that serves as the second messenger of electrical signals to initiate many cellular events, including muscle contraction, neurotransmitter release, and gene expression (1). The pore-forming component of VGCCs is provided by the α_1 subunit, a protein of about 2000 amino acid residues (2). This subunit contains four structurally conserved domains (I–IV), each of which contains six transmembrane segments (S1–S6) and a membrane-associated loop between S5 and S6 (called the pore loop or P-loop). The voltage sensitivity of VGCCs and structurally related cation channels is conveyed by the S4 segments, which contain several positively charged residues. S2 and S3 contain conserved negative charges that are likely to interact electrostatically with the positively charged residues of S4. The S5-P-loop-S6 region forms the pore domain (see Fig. 1).

Mutations in the α_1 subunits resulting in structural aberrations cause hereditary diseases (called Ca^{2+} channelopathies) in mammals, such as incomplete congenital stationary night blindness, hypokalemic periodic paralysis, episodic ataxia type 2 and familial hemiplegic migraine in humans, and ataxia and seizures in mice (3–6). Most of the mutations are predicted to produce truncated α_1 subunits with no significant channel activity by introducing a premature stop codon or leading to aberrant splicing. Single missense mutations can also result in the production of complete or partial loss-of-function subunits and these mutation sites are likely to be restricted to amino acid residues at transmembrane segments or loops known to be important for channel activity (7–9).

A eukaryotic model organism, the yeast *Saccharomyces cerevisiae*, carries only one gene (designated *CCH1*) coding for a protein structurally homologous to the animal α_1 subunits of VGCCs. Physiologically, the Cch1 protein is necessary for mating pheromone-induced Ca^{2+} uptake (10–13), store-operated Ca^{2+} entry (14), endoplasmic reticulum stress-induced Ca^{2+} uptake (15), and a hyperosmotic stress-induced increase in cytosolic Ca^{2+} concentration (16).

* This work was supported by grants from CREST, Japan Science and Technology Agency (to H. I.), a Grant-in-Aid for Scientific Research on Priority Areas No. 15031212 (to H. I.) and Grant-in-Aid for Scientific Research B No. 16370072 (to H. I.) from the Ministry of Education, Culture, Sports, Science and Technology in Japan. The costs of publication of this article were defrayed in part by the payment of page charges. This article must therefore be hereby marked "*advertisement*" in accordance with 18 U.S.C. Section 1734 solely to indicate this fact.

[S] The on-line version of this article (available at http://www.jbc.org) contains supplemental Fig. S1.

[1] Both authors contributed equally to this work.

[2] Present address: Picower Institute for Learning and Memory, Massachusetts Institute of Technology, Cambridge, MA 02139.

[3] Present address: Science and Technology Foresight Center, National Institute of Science and Technology Policy, 5-1 Marunouchi 2 chome, Chiyoda-ku, Tokyo 100-0005, Japan.

[4] To whom correspondence should be addressed: Dept. of Biology, Tokyo Gakugei University, 4-1-1 Nukui kita-machi, Koganei-shi, Tokyo 184-8501, Japan. Tel.: 81-42-329-7517; Fax: 81-42-329-7517; E-mail: iida@u-gakugei.ac.jp.

[5] The abbreviations used are: VGCC, voltage-gated Ca^{2+} channel; EGFP, enhanced green fluorescent protein; CMV, cytomegalovirus; BHK, baby hamster kidney; ORF, open reading frame.

When exposed to the mating pheromone α-factor, mutants lacking *CCH1* die because of a deficiency in Ca^{2+} uptake (10, 11). This phenotype, as well as the Ca^{2+} uptake ability, was used to assess the activity of wild-type and mutant Cch1 proteins in this study. To gain channel activity, Cch1 requires another protein, Mid1, as revealed by genetic analyses (10, 11, 13). Mid1 has no structural homologue in higher eukaryotes (17), but has stretch-activated Ca^{2+} channel activity when expressed in mammalian cells (18, 19). There is no orthologue of genes encoding the auxiliary subunits $\alpha_2\delta$, β, and γ of mammalian VGCCs in the *S. cerevisiae* genome.

rbCII is a member of an L-type VGCC α_1 subunit subfamily, $Ca_v1.2$, isolated from the rat brain (20, 21), and has been used in this study as a mammalian counterpart of yeast Cch1 to attempt to generalize findings with Cch1. The activity of rbCII has been successfully analyzed when it is transfected in baby hamster kidney BHK6 cells that stably express rabbit β_{1a} and α_2/δ necessary for efficient targeting of α_1 to the plasma membrane (22, 23).

Here, we report that a mutant allele of yeast *CCH1*, formerly designated *mid3-1* (17), has a missense mutation causing a Gly^{1265} to Glu substitution that results in a complete loss-of-function. The glycine residue is located in the cytoplasmic linker between the S2 and S3 segments in domain III, completely conserved during evolution, and proven to be important as being the smallest residue volume. In addition, we show that the Gly residue is not only important for Cch1 function, but also for rbCII channel activity. Because attention has never been focused on the Gly residue in this linker of any VGCC, our finding should help elucidate the structure-function relationships of VGCCs.

EXPERIMENTAL PROCEDURES

Yeast Strains and Media—The parental strain H207 (*MAT***a** *his3-Δ1 leu2–3,112 trp1–289 ura3–52 sst1–2*) and its derivative mutant strains H3031 (*MAT***a** *cch1-1* (formerly *mid3-1*) *his3-Δ1 leu2–3,112 trp1–289 ura3–52 sst1–2*) and H314 (*MATα cch1Δ::TRP1 his3-Δ1 leu2–3,112 trp1–289 ura3–52 sst1–2*) were described previously (13, 17). To construct H317 (*MAT***a** *cch1Δ::HIS3 his3-Δ1 leu2–3,112 trp1–289 ura3–52 sst1–2*), a *CCH1* knock-out plasmid pCCH1DH (see below) was cut with EcoRI and SphI and introduced into H207. Successful disruption of the *CCH1* gene was confirmed by PCR analysis with Ex *Taq* polymerase (Takara Bio Inc., Otsu, Japan). The strains X2180-1A, A364A, KA31-1A, YPH500, and S173-6B were described previously (17, 24–26). Rich medium YPD and synthetic media SD and SD.Ca100 were prepared as described previously (17). The SD.Ca100 medium contained 100 μM $CaCl_2$, whereas SD contained 681 μM $CaCl_2$.

DNA Sequencing—The *CCH1* gene of various strains was amplified by PCR with LA *Taq* polymerase (Takara Bio Inc.) using the primers 5′-200F-EcoKpn and 3′-305R-Sph, listed in Table 1. The resulting 6.6-kb DNA fragments were directly sequenced with BigDye Terminator version 3.1 cycle sequencing kit (Applied Biosystems, Foster City, CA).

Construction of Plasmids—The plasmids used in this study were listed in Table 2. The promoter of *CCH1* (P_{CCH1}, 200 bp), its ORF (*CCH1* ORF, 6,120 bp), and the terminator (T_{CCH1}, 305 bp) were amplified by PCR with LA *Taq* polymerase using the genomic DNA of H207 or X2180-1A cells as a template. The PCR primers and an adaptor are listed in Table 1.

To construct pCCH1D, a pUC18-derived plasmid carrying P_{CCH1} and T_{CCH1}, the PCR-amplified promoter and terminator fragments of the *CCH1* gene of H207 were cut with appropriate restriction enzymes and inserted into the multicloning site of pUC18, then an adaptor, which contains a stop codon and an XhoI site, was inserted between P_{CCH1} and T_{CCH1}. The *CCH1* knock-out plasmid pCCH1DH was constructed by inserting the *HIS3*-containing 1.8-kb BamHI-XhoI fragment of pJJ215 (27) between P_{CCH1} and T_{CCH1} of pCCH1D.

To clone the *CCH1* gene in *Escherichia coli*, we first constructed a new *S. cerevisiae-E. coli* shuttle vector (named pBC111), which replicates with a low copy number in *E. coli*, by replacing the ColE1 *ori* of YCplac111 (28) with the ColE1 *ori* and the *rop* gene of pBR322, as follows. pBR322 was cut with SalI and MscI and the overhangs were filled-in using a DNA blunting kit (Takara Bio Inc.). The larger fragment was self-ligated and the SalI site that remained was destroyed by a series of SalI-cut, fill-in, and self-ligation. The 2.9-kb AatII-SphI fragment of the resulting plasmid was ligated with the 3.9-kb SphI-AatII fragment of YCplac111 to produce pBC111. pBCS111 and pBCT111 are derivatives of pBC111, each of which carries P_{CCH1}-T_{CCH1} or P_{TDH3}-T_{ADH1}, respectively. pBCS111 was constructed by inserting the 0.5-kb EcoRI-SphI fragment of pCCH1D into the multicloning site of pBC111. To construct pBCT111, P_{CCH1} and T_{CCH1} of pBCS111 were replaced with the P_{TDH3}-containing 0.7-kb EcoRI-BamHI fragment of pUGPD (29) and the T_{ADH1}-containing 0.3-kb PstI-SphI fragment of pGBKT7 (Clontech, Palo Alto, CA), respectively. The PCR-amplified *CCH1* ORF derived from H207 or H3031 was cut with BamHI and SalI and inserted between the BamHI and SalI sites of pBCS111 or pBCT111. The resulting plasmids were designated pBCS-CCH1H or pBCS-CCH1Hm1 and pBCT-CCH1H or pBCT-CCH1Hm1, respectively. Recombinant Cch1 proteins expressed from these plasmids have three additional amino acid residues (Val, Asp, and Thr) at the carboxyl terminus. The plasmids, pBCT-CCH1H-EGFP or pBCT-CCH1Hm1-EGFP, used to express EGFP-tagged Cch1 proteins were constructed by inserting the 0.6-kb NcoI (blunted)-NotI fragment of pEGFP (Clontech) between the SalI (blunted) and NotI sites of pBCT-CCH1H or pBCT-CCH1Hm1, respectively.

pBCMS-EGFP, a low-copy derivative of the mammalian expression plasmid pCMS-EGFP (Clontech) was constructed as follows. The restriction sites spanning from SphI to XbaI of the multicloning site of pBC111 were deleted, and the 2.9-kb AatII (blunted)-BamHI fragment of the resulting plasmid was inserted between the BglII and ApaLI (blunted) sites of pCMS-EGFP. rbCII cDNA (kindly gifted by Dr. T. P. Snutch; see Refs. 20 and 21) was inserted between the MluI and SalI sites of the multicloning site of pBCMS-EGFP. The resulting plasmid, pBCMS-EGFP-rbCII, was used to transiently express rbCII under the control of the immediate-early promoter/enhancer of cytomegalovirus (CMV promoter) in BHK6 cells.

TABLE 1
Oligonucleotides used in this study
Underlines represent the entirety or a part of restriction sites. Boxed triplets show the initiation or termination codon.

Usage	Name	Sequence
PCR primers		
Promoter	5'-200F-EcoKpn	5'-GGGAATTCGGTACCGAAGGTTCCTGTTCACAGAGGAAT-3'
	5'R-Bam	5'-GGGGATCCAGTACTAACAATATATTCTATTTAGTAATG-3'
Terminator	3'F-Pst	5'-CCCTGCAGTAAATTATATAAGGGCATATTTAAGAGG-3'
	3'-305R-Sph	5'-GGGCATGCCCTTCTAATGGGTACTCTTGCAATG-3'
ORF	5'F-Bam	5'-GGGATCCATGCAGGGGAGAAAAAGGACGCT-3'
	3'R-Sal	5'-GGGTCGACTCTATCAATTAGATCATTTGCGCTATC-3'
Cc-peptide	Cc-5'F-Bam	5'-GGGGATCCACAAGATGGAAATTTCATTGCAGGATG-3'
	Cc-3'R-Sal	5'-GGTCGACTTATCTATCAATTAGATCATTTGCGCTA-3'
Mutagenesis	3298F	5'-TCACTAAAAAGGCTGAGAATGTTTGCT-3'
	3999R	5'-CATAACTAGGTTAAATGTTTGAC-3'
	G1265S-F*	5'-CAGTAGCTGACTCATTTATATATTCTCC-3'
	G1265S-R*	5'-GGAGAATATATAAATGAGTCAGCTACTG-3'
	G959E-F*	5'-CCTTAAGATGACTGCTTACGAGGCTTTCCTGC-3'
	G959E-R*	5'-GCAGGAAAGCCTCGTAAGCAGTCATCTTAAGG-3'
***SalI/XhoI/PstI* Adaptor**		5'-TCGACACGTAGCTCGAGCTGCA-3'
(double strand)		3'-GTGCATCGAGCTCG-5'

[a] Asterisk, The G1265S-F and G1265S-R were used to substitute Ser for the Gly^{1265} of Cch1, and the G959E-F and G959E-R were used to substitute Glu for the Gly^{959} of rbCII, for example. The doubly underlined triplets in these oligonucleotides were changed to appropriate nucleotides to substitute the corresponding amino acid for Gly^{1265} or Gly^{959}. Boldfaces indicates the changed nucleotides.

TABLE 2
Plasmids used in this study

Plasmid	Characteristics	Source
***E. coli* plasmids**		
pCCH1D	P_{CCH1} T_{CCH1} in pUC18	This study
pCCH1DH	P_{CCH1} *HIS3* T_{CCH1} in pUC18	This study
Expression plasmids		
YCplac111	ColE1-*ori ARS1 CEN4 LEU2*	Gietz and Sugino (28)
pBC111[a]	ColE1-*ori-rop* in YCplac111	This study
pBCS111	P_{CCH1} T_{CCH1} in pBC111	This study
pBCS-CCH1H[b]	*CCH1H* ORF in pBCS111	This study
pBCS-CCH1Hm1[b]	*cch1-1* ORF in pBCS111	This study
pBCT111	P_{TDH3} T_{ADH1} in pBC111	This study
pBCT-CCH1H[b]	*CCH1H* ORF in pBCT111	This study
pBCT-CCH1Hm1[b]	*cch1-1* ORF in pBCT111	This study
pBCT-CCH1H-EGFP[b]	*CCH1H-EGFP* ORF in pBCT111	This study
pBCT-CCH1Hm1-EGFP[b]	*cch1-1-EGFP* ORF in pBCT111	This study
pBCMS-EGFP[a]	ColE1-*ori-rop* P_{CMV}-EGFP marker	This study
pBCMS-EGFP-rbCII	rbCII cDNA in pBCMS-EGFP	This study

[a] The ColE1 *ori* of YCplac111 and pCMS-EGFP have been replaced with a DNA fragment containing the ColE1 *ori* and the *rop* gene derived from pBR322.
[b] The suffixes of CCH1, *i.e.* H and Hm1, represent the *CCH1* and *cch1-1* ORFs derived from the strains H207 (*CCH1*) and H3031 (*cch1-1*), respectively.

In Vitro Site-directed Mutagenesis—In vitro site-directed mutagenesis was performed using the two-step PCR method reported by Higuchi *et al.* (30). The PCR primers are listed in Table 1. pBCT111 plasmids bearing various *cch1* mutant genes were constructed by replacing the 0.4-kb KpnI-ApaI fragment of pBCT-CCH1H with the corresponding fragment that had been produced by PCR-based, *in vitro* site-directed mutagenesis, and the nucleotide sequence was verified. pBCS111 plasmids bearing the same *cch1* mutant genes were constructed by replacing the 4.1-kb SacI-SalI fragment of pBCS-CCH1H with the corresponding fragment of the pBCT111 bearing the *cch1* mutant genes constructed as described above.

In the case of rbCII, QuikChange II XL Site-directed Mutagenesis Kit (Stratagene, La Jolla, CA) was used to mutagenize the rbCII cDNA subcloned in pBluescript II SK(−). The 1.4-kb SpeI-EcoRV fragment of the wild type cDNA was replaced with each mutated fragment, and each

mutated full-length cDNA was introduced into pBCMS-EGFP after the nucleotide sequence was verified.

Preparation of Polyclonal Anti-Cch1 Antibodies—A PCR fragment encoding the Cch1 carboxyl-terminal peptide spanning from amino acid residue 1,949 to 2,039 was cut with BamHI and SalI and inserted into pQE30 (Qiagen Inc., Valencia, CA) to be conjugated with a His_6 tag at the amino terminus. The His_6-tagged carboxyl-terminal peptide was purified from an *E. coli* transformant (strain JM109) carrying this plasmid using nickel-nitrilotriacetic acid-agarose beads (Qiagen Inc.) under denaturing conditions. Affinity purified rabbit antibodies against this peptide were prepared by Promega Co. (Madison, WI).

Western Blotting and Fluorescence Microscopy—Western blotting was carried out according to the method described previously (17) except that SDS-PAGE samples were heated for 3 min at 70 °C. The affinity purified rabbit polyclonal antibodies against the carboxyl-terminal peptide described above were used at a concentration of 0.07 μg/ml to detect the wild-type and various mutant forms of the Cch1 protein. Fluorescence microscopy on cells expressing the Cch1G1265E-EGFP and Cch1-EGFP was performed as described previously (31).

Determination of the Viability of Yeast Cells—The viability of cells exposed to 6 μM α-factor in SD.Ca100 medium was determined using the methylene blue liquid method (24).

Determination of Ca^{2+} Accumulation in Yeast Cells—Exponentially growing cells in SD.Ca100 medium were incubated for 2 h with 6 μM α-factor and 185 kBq/ml (1.85 kBq/nmol) of $^{45}CaCl_2$ (PerkinElmer Life Sciences). Samples were taken, filtered through Millipore filters (type HA; 0.45 μm) that had been presoaked in 5 mM $CaCl_2$, and washed five times with the same solution. The radioactivity retained on the filters was counted with a scintillation mixture, ReadyProtein (Beckman Japan, Tokyo), in a liquid scintillation counter.

Electrophysiological Recordings—Electrophysiological recordings were performed in the whole cell patch clamp configuration using Patch/Whole Cell Clamp Amplifier Axopatch 200B (Axon Instruments, Foster City, CA) and A/D converter (Digidata 1200, Axon Instruments). Data acquisition was performed by using pCLAMP7 software (Axon Instruments). Capacitative components were electrically compensated. Leak subtraction was performed with P/N method (N = 4–6). All experiments were performed at room temperature.

Ba^{2+} currents (I_{Ba}) through Ca^{2+} channels exogenously expressed in BHK6 cells were measured as described previously (22). The external solution contained 137 mM NaCl, 5.4 mM KCl, 1 mM $MgCl_2$, 10 mM HEPES, 10 mM glucose, and 2 mM $BaCl_2$ (pH adjusted to 7.4 with NaOH at room temperature). The resistance of the recording pipettes was 2–2.5 MΩ when filled with the pipette solution containing 120 mM $CsMeSO_4$, 20 mM tetraethyl ammonium chloride, 14 mM EGTA, 5 mM Mg-ATP, 5 mM Na_2 creatine phosphate, 0.2 mM GTP, and 10 mM HEPES (pH 7.3 adjusted with CsOH at room temperature).

Immunohistochemistry—BHK6 cells were fixed in 4% formaldehyde for 10 min, permeabilized with 1% Triton X-100 in phosphate-buffered saline, and blocked with TBS-T solution (20 mM Tris-HCl, 137 mM NaCl, 0.01% Tween 20, pH 7.4) containing 0.25 mg/ml bovine serum albumin for 1 h at room temperature. Polyclonal antibodies against $Ca_V1.2$ (rabbit anti CNC1 (ACC-003, Alomone Labs, Jerusalem, Israel) or rat anti-CNC1 (custom made)) were visualized with secondary antibodies labeled with Alexa Fluor 543 or Alexa Fluor 633 (Invitrogen). Images were acquired by confocal microscopy (LSM-510 META, Carl Zeiss, Inc., Oberkochen, Germany) and presented in supplemental materials Fig. S1.

Statistical Analysis—Statistical significance was determined using the unpaired Student's *t* test with a *p* value <0.05 required for significance.

TABLE 3
Amino acid variation and mutation in the Cch1 protein
The nucleotides changed in the strains H207, A364A, and H3031 are underlined.

Amino acid position (nucleotide position)	Strain (genotype)		
	X2180-1A, S288C, YPH500, KA31-1A, S173-6B	H207, A364A	H3031
	(CCH1)	*(CCH1)*	*(cch1-1)*
765 (2,294)	Gly (GGA)	Ala (GCA)	Ala (GCA)
882 (2,646)	Asn (AAT)	Lys (AAA)	Lys (AAA)
972 (2,914)	Thr (ACT)	Ala (GCT)	Ala (GCT)
1,117 (3,351)	Asp (GAC)	Asp (GAT)	Asp (GAT)
1,265 (3,794)	Gly (GGA)	Gly (GGA)	Glu (GAA)[a]
1,413 (4,238)	Ser (AGT)	Asn (AAT)	Asn (AAT)
1,607 (4,819)	Met (ATG)	Val (GTG)	Val (GTG)
1,627 (4,879)	Phe (TTT)	Val (GTT)	Val (GTT)

[a] The only mutation found in the *cch1-1* allele.

RESULTS

Genetic Characterization of a cch1 Allele of S. cerevisiae—The phenotypes of the previously reported *mid3-1* recessive mutant are essentially the same as those of the *cch1*Δ mutant: these include mating pheromone-induced death, low Ca^{2+} uptake activity, and low viability in the stationary phase. In addition, the corresponding genes have not been cloned despite numerous trials (11, 13). These features prompted us to perform genetic analysis on them. The two mutants were crossed (*MAT***a** *mid3-1* × *MATα cch1*Δ) and the resulting diploids showed low viability in the stationary phase, like *mid3-1* and *cch1*Δ haploids, suggesting that the two alleles belong to the same complementation group. The diploids were sporulated and subjected to tetrad analysis (32). All cells germinated from 72 spores dissected from 18 asci again showed low viability in the stationary phase. In addition, all the *MAT***a** cells from each spore (a total of 36 spores) showed the mating pheromone-induced death phenotype. These results indicate that *mid3-1* is allelic to *cch1*Δ. We therefore renamed *mid3-1* to *cch1-1*.

PCR products, synthesized using genomic DNA as a template of the *cch1-1* mutant (strain H3031) as well as of the parental strain H207 (*CCH1*), were directly sequenced. Three independent PCR products for each strain were sequenced to avoid misinterpretation due to possible PCR errors. Consequently, we identified a missense mutation (G3794A) in *cch1-1*, which results in a substitution of glutamate (Glu) for glycine (Gly) at codon 1,265 (G1265E) (Table 3).

We noted a strain-dependent polymorphism in *CCH1*. Seven nucleotides and six encoded amino acids in *CCH1* of the strain

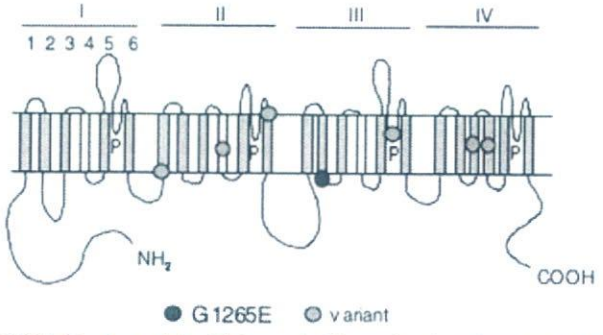

FIGURE 1. **Structure of the Cch1 protein.** The predicted topology of Cch1 and the location of the G1265E mutation (*red circle*) and strain-dependent amino acid variations (*blue circle*) are shown. For details of the amino acids and codons, see Table 3. Roman numerals *I–IV* represent putative domains and the Arabic numerals *1–6* putative transmembrane segments (S1–S6). The putative S4 segments in domains I–III, containing repeated motifs of a positively charged residue followed by two hydrophobic residues, are *colored yellow*. The putative S4 segment of domain IV lacks the motifs. *P* represents the putative pore loop. The amino and carboxyl termini are located in the cytoplasm.

H207 we determined were different from those of *CCH1* of the strain S288C listed in the *Saccharomyces* Genome Data base (www.yeastgenome.org) (Table 3). Because S288C is isogenic to a standard laboratory yeast strain, X2180-1A, we determined the *CCH1* nucleotide sequence of X2180-1A and four other standard laboratory strains and found that H207 shares the same nucleotide sequence with one strain and that X2180-1A and S288C share the same sequence with three other strains (Table 3). It is notable that the viability of X2180-1A cells was as high as that of H207 cells after exposure to α-factor (data not shown), suggesting that the six amino acid variations do not affect Cch1 function.

To confirm that the G1265E mutation is the only determinant for the phenotypes of the *cch1-1* mutant, we first developed a new vector of low copy number in *E. coli* (designated pBC111) because cloning of *CCH1* has long been impossible due to the probable toxicity of this gene or protein for *E. coli* (11, 13). pBC111 is an *E. coli*-yeast shuttle vector having the ColE1-*ori-rop* sequence ensuring 15–20 copies per *E. coli* cell and an *S. cerevisiae* centromere ensuring 1–3 copies per *S. cerevisiae* cell. Using this, we generated the G1265E mutation in *CCH1* cloned from X2180-1A and the resulting mutant gene was tested for its ability to rescue the mating pheromone-induced death phenotype and low Ca^{2+} uptake activity of the *cch1*Δ mutant. The results showed that this mutant gene did not rescue the two phenotypes at all, just like the G1265E mutant gene of H207 (data not shown), indicating that the two phenotypes are attributed to the G1265E mutation only. We therefore used the *CCH1* alleles based on the H207 background hereafter and designated the mutant Cch1 protein with the G1265E mutation Cch1G1265E.

Gly^{1265} Is Completely Conserved—Based on a conventional transmembrane domain prediction (33), Gly^{1265} was predicted to be located in the cytoplasmic linker connecting the putative transmembrane segments S2 and S3 of domain III (Fig. 1), although this residue is alternatively predicted to be included in the S2 segment by other methods, such as SGD (www.yeastgenome.org) and UniProt (www.expasy.uniprot.org). Here, we followed the conventional prediction (33). To explore the importance of the glycine residue in the domain III S2–S3 linker, we compared the amino acid sequences of the corresponding linker of the VGCC family. Fig. 2 shows a multiple amino acid sequence alignment of the linker and its neighbors of a total of 58 VGCCs and candidates from 17 species, including humans, yeasts, and representative model organisms, such as mice, rats, zebrafish, fruit flies, and nematodes. This alignment clearly indicates that the glycine residue is completely conserved from yeasts to humans. The finding prompted us to investigate the importance of the Gly^{1265} of Cch1 because the glycine residue has never been investigated in any VGCC or candidate, although it is remarkably conserved during evolution.

The G1265E Mutation Results in a Complete Loss of Function—There are three possibilities for the inability of the Cch1G1265E protein in cellular function: loss-of-function, instability, and lack of plasma membrane targeting. To examine these possibilities, we first investigated the amount of the Cch1 and Cch1G1265E proteins by Western blotting and found that the amount of Cch1G1265E produced from the *cch1-1* gene was slightly smaller than that of the wild-type Cch1 protein (Fig. 3*A*, *left panel*). However, this decrease is unlikely to be the cause of the defect of Cch1G1265E because an ~20-fold overproduction of Cch1G1265E under the control of a strong *TDH3* promoter (Fig. 3*A*, *left panel*) did not rescue the decreased viability and Ca^{2+} uptake activity of the *cch1*Δ mutant at all (Fig. 3, *B* and *C*). Thus, a putative instability of the Cch1G1265E protein does not account for its inability in cellular function.

We then examined the subcellular localization of Cch1G1265E, tagged with green fluorescence protein (Cch1G1265E-EGFP) produced under the *TDH3* promoter on a centromere plasmid, using fluorescence microscopy and found that Cch1G1265E-EGFP was normally localized to the plasma membrane and the endoplasmic reticulum membrane-like structure (Fig. 3*D*). Note that the amount of Cch1-EGFP and Cch1G1265E-EGFP produced under the self-promoter on a centromere plasmid was too small to visualize their fluorescence images (13).

We also found that the 20-fold overproduction of Cch1G1265E in the *CCH1* strain (Fig. 3*A*, *right panel*) resulted in only a small decrease in both the viability and Ca^{2+} uptake activity (Fig. 3, *E* and *F*). This result is consistent with the genetic data that the *cch1-1* (*mid3-1*) mutation is recessive (17) and indicates that the interferential effect of Cch1G1265E on wild-type Cch1 is small. Taken together, we conclude that the G1265E mutation results in a complete loss-of-function of Cch1, not its instability and mislocalization.

Importance of Gly^{1265} as the Smallest Amino Acid Residue—We next investigated the cause of the complete loss-of-function of the Cch1G1265E protein. One can speculate three possibilities for the cause: a negative charge, hydrophilicity, or a large residue volume of glutamate compared with glycine. To examine these possibilities, we systematically substituted nine amino acids with different chemical and physical properties for Gly^{1265}, introduced the resulting mutant genes on a centromere plasmid into the *cch1*Δ mutant, and examined their activity by cell viability and Ca^{2+} uptake assays (Fig. 4).

Species	Protein	Type	NCBI-GI No.	Length aa	Sequence
H. sapiens	$Ca_v1.1$ (α_{1S})	L	NP_000060	1873	831- ILKHFDIGFTSVFTVEIVLKMTTYGAFLHKGSFCRNYFNMLDLLVVAVSLI
	$Ca_v1.2$ (α_{1C})	L	NP_000710	2138	932- ILFYFDIVFTTIFTIEIALKMTAYGAFLHKGSFCRNYFNILDLLVVSVSLI
	$Ca_v1.3$ (α_{1D})	L	NP_000711	2181	938- ILGYFDYAFTAIFTVEILLKMTTFGAFLHKGAFCRNYFNLLDMLVVGVSLV
	$Ca_v1.4$ (α_{1F})	L	NP_005174	1977	903- ILGYFDYAFTSIFTVEILLKMTVFGAFLHRGSFCRSWFNMLDLLVVSVSLI
	$Ca_v2.1$ (α_{1A})	P/Q	NP_000059	2261	1276- VLRYFDYVFTGVFTFEMVIKMIDLGLVLHQGAYFRDLWNILDFIVVSGALV
	$Ca_v2.2$ (α_{1B})	N	NP_000709	2339	1182- ALKYLDYIFTGVFTFEMVIKMIDLGLLLHPGAYFRDLWNILDFIVVSGALV
	$Ca_v2.3$ (α_{1E})	R	NP_000712	2270	1185- VLRYFDYVFTGVFTFEMVIKMIDQGLILQDGSYFRDLWNILDFVVVVGALV
	$Ca_v3.1$ (α_{1G})	T	NP_061496	2377	1309- FLTLSNYIFTAVFLAEMTVKVVALGWCFGEQAYLRSSWNVLDGLLVLISVI
	$Ca_v3.2$ (α_{1H})	T	NP_001005407	2347	1327- FLSVSNYIFTAIFVAEMMVKVVALGLLSGEHAYLQSSWNLLDGLLVLVSLV
	$Ca_v3.3$ (α_{1I})	T	NP_001003406	2188	1168- FLTVSNYIFTAIFVGEMTLKVVSLGLYFGEQAYLRSSWNVLDGFLVFVSII
	VGCNL1[1]	?	NP_443099	1738	917- TLQIAEYVFVIFMSIELNLKIMADGLFFTPTAVIRDFGGVMDIFIYLVSLI
O. cuniculus	$Ca_v1.1$ (α_{1S})	L	AAA31159	1873	831- ILGYFDIAFTSVFTVEIVLKMTTYGAFLHKGSFCRNYFNILDLLVVAVSLI
	$Ca_v2.1$ (α_{1C})	L	P15381	2171	962- ILFYFDIVFTTIFTIEIALKMTAYGAFLHKGSFCRNYFNILDLLVVSVSLI
	$Ca_v2.1$ (α_{1A})	P/Q	P27884	2424	1285- VLRYFDYVFTGVFTFEMVIKMIDLGLVLHQGAYFRDLWNILDFIVVSGALV
	$Ca_v2.1$ (α_{1B})	N	Q05152	2339	1187- ALKYMDYIFTGVFTFEMVIKMIDLGLLLHPGAYFRDLWNILDFIVVSGALV
	$Ca_v2.1$ (α_{1E})	R	Q02343	2259	1175- VLRYFDYVFTGVFTFEMVIKMIDQGLILQDGSYFRDLWNILDFVVVVGALV
M. musculus	$Ca_v1.1$ (α_{1S})	L	XP_358335	1807	955- ILEYFDYVFTAVFTVEIVLKMTTYGAFLHKGSFCRNYFNILDLLVVAVSLI
	$Ca_v1.2$ (α_{1C})	L	NP_033911	2139	932- ILGNADYVFTSIFTLEIILKMTAYGAFLHKGSFCRNYFNILDLLVVSVSLI
	$Ca_v1.3$ (α_{1D})	L	NP_083257	2166	940- ILGYFDYAFTAIFTVEILLKMTTFGAFLHKGAFCRNYFNLLDMLVVGVSLV
	$Ca_v1.4$ (α_{1F})	L	NP_062528	1985	908- ILGYFDYAFTSIFTVEILLKMTVFGAFLHRGSFCRSWFNMLDLLVVSVSLI
	$Ca_v2.1$ (α_{1A})	P/Q	NP_031604	2164	1179- VLRYFDYVFTGVFTFEMVIKMIDLGLVLHQGAYFRDLWNILDFIVVSGALV
	$Ca_v2.2$ (α_{1B})	N	NP_031605	2288	1170- ALEYMDYIFTGVFTCEMVIKMIDLGLLLHPGAYFRDLWNILDFIVVSGALV
	$Ca_v2.3$ (α_{1E})	R	NP_033912	2272	1188- VLRYFDYVFTGVFTFEMVIKMIDQGLILQDGSYFRDLWNILDFVVVVGALV
	$Ca_v3.1$ (α_{1G})	T	NP_033913	2295	1310- FLTLSNYIFTAVFLAEMTVKVVALGWCFGEQAYLRSSWNVLDGLLVLISVI
	$Ca_v3.2$ (α_{1H})	T	NP_067390	2359	1338- FLSVSNYIFTAIFVVEMMVKVVALGLLWGEHAYLQSSWNVLDGLLVLVSLV
R. norvegicus	$Ca_v1.2$ (α_{1C};rbCII)	L	AAA18905	2143	935- ILGNADYVFTSIFTLEIILKMTAYGAFLHKGSFCRNYFNILDLLVVSVSLI
	$Ca_v1.2$ (α_{1C})	L	NP_036649	2169	962- ILFYFDIVFTTIFTIEIALKMTAYGAFLHKGSFCRNYFNILDLLVVSVSLI
	$Ca_v1.3$ (α_{1D})	L	NP_058994	2203	977- ILGYFDYAFTAIFTVEILLKMTTFGAFLHKGAFCRNYFNLLDMLVVGVSLV
	$Ca_v1.4$ (α_{1F})	L	NP_446153	1981	902- ILGYFDYAFTSIFTVEILLKMTVFGAFLHQGSFCRSWFNLLDLLVVSVSLI
	$Ca_v2.1$ (α_{1A})	P/Q	NP_037050	2212	1227- VLRYFDYVFTGVFTFEMVIKMIDLGLVLHQGAYFRDLWNILDFIVVSGALV
	$Ca_v2.2$ (α_{1B})	N	NP_671482	2333	1179- ALKYMDYIFTGVFTFEMVIKMIDLGLLLHPGAYFRDLWNILDFIVVSGALV
	$Ca_v2.3$ (α_{1E})	R	NP_062167	2222	1137- VLRYFDYVFTGVFTFEMVIKMIDQGLILQDGSYFRDLWNILDFVVVVGALV
	$Ca_v3.1$ (α_{1G})	T	NP_113789	2254	1288- FLTLSNYIFTAVFLAEMTVKVVALGWCFGEQAYLRSSWNVLDGLLVLISVI
	$Ca_v3.2$ (α_{1H})	T	AAG35187	2359	1338- FLSVSNYIFTAIFVVEMMVKVVALGLLWGEHAYLQSSWNVLDGLLVLVSLV
	$Ca_v3.3$ (α_{1I})	T	NP_064469	1835	1162- FLTVSNYIFTAIFVGEMTLKVVSLGLYFGEQAYLRSSWNVLDGFLVFVSII
	VGCNL1[1]	?	NP_705894	1737	917- TLQIAEYVFVIFMSIELNLKIMADGLFFTPTAVIRDFGGVMDIFIYLVSLI
G. gallus	ChCaChA1D (α_{1B})	L	AAC08304	2190	939- ILGYADYVFTSMFTFEIILKMTAFGAFLHKGSFCRNYFNLLDLLVVGVSLV
D. rerio	cacna1s (α_{1S})	L	NP_99989	1847	851- VLAYADIVFTTVFTIEIVLKMTVYGAFLHPGSFCRNSFNILDLIVVAVSLL
	cacna1c (α_{1C})	L	NP_571975	2168	944- ILGYADYVFTGIFTIEIILKMTAYGAFLHKGSFCRNYFNILDLVVVSVSLI
	cacna1d (α_{1D})	L	NP_982351	2082	861- ILGYFDYAFTAIFTVEIVLKMTTYGAFLHKGAFCRNYFNLLDLLVVGVSLV
L. bleekeri	VDCC[2]-α_1	?	BAA13136	2196	927- ILNYFDYVFTGVFTIEMLLKIVDLGIILHPGSYCRDAWNILDATVVICALV
D. melanogaster	Ca-alpha1D	L	AAF53504	2516	1376- VLNKFDYFFTAVFTIELILKLISYGFVLHDGAFCRSAFNLLDLLVVCVSLI
	cac[3]	P/Q	AAF48120	1848	801- ILNYFDYAFTGVFTIEMLLKIVDLGVILHPESSFNRFDCVVISGSIFEVIW
	Ca-alpha1T	T	AAF46127	2893	1883- FLATANYVFTVVFTVEMFIKVVATGMFYGHDAYFTSGWNIMDGSLVTISII
	na[4]	?	AAF48365	2196	1217- TLQIAEYGFVIFMSLFLALKILADGLFFTPKAYIKDVAAALDVFIYVVSTS
C. elegans	egl[5]-19	L	AAM75372	1877	830- ILNYFDYFFTSVFTVEIILKVIVFGLVFHKGSFCRNAFNLLDILVVAVSLT
	unc[6]-2	P/Q	AAP82640	2027	886- VLQYMDYCFTGVFACEMLLKLIDQGILLHPGSYCRDFWNILDGIVVTCALF
	cca[7]-1	T	AAM51535	1837	1144- FLHISGYIFTVIFTGEMMMKVIANGCFIGQAAYFKDGWNILDGILVVISLI
	nca[8]-1	?	AAM81121	1913	1047- YLQISDYFFVLSMTFELCVKIIANGLFFTPKAVVRDVGGVMNLFIYFTSVI
	nca[8]-2	?	AAA81424	1785	958- YLQIAEYIFVLVMSFELIVKCIANGLFFTPKALVTDVGDILTIFIYITSLM
N. crassa	hypothetical	?	XP_331961	2218	1242- WFRWVDTGFAIVFTLEALIKVIADGFLWTPNAYFRSTWGVIDAIVLITLWI
M. grisea	hypothetical	?	XP_360269	2128	1215- WFVWTDMAFAAIFTTEAFIKVIADGFFFTPNAYFRSSWGLIDAVVLTTLWI
A. nidulans	calcium channel	?	AAL37946	2110	1223- WFTYTDLGFAILFSIEALIKVIADGFFWTPNAYFRGSWGFIDGIVLVTLWI
C. neoformans	hypothetical	?	AAW42868	2028	1202- WFDLTEVTLGLIFVLEAAMKIVADGFIFAPNAYLLSLWNVLDFIILITLLI
S. pombe	VIC[9]	?	NP_593894	1854	979- WFVWTEVAFATIFTIEAAIKIIADGFCITPNAYLRSTWNCIDFFVLVTLWI
C. albicans	Cch1	?	AAN86029	2254	1366- WVFWAEFVFVMVFTVEFAIKVIADGFIFTPNAYTRSSWNLIDFVVLLSLWI
A. gossypii	calcium channel	?	NP_983261	1963	1165- WLNVCECTFVALFTLEFLIKTIADGFLYSPNAYINNPWNCIDLVVLISMWI
S. cerevisiae	Cch1	?	NP_011733	2039	1241- WSSALDGAFIGAFSIEFIVKTVADGFIYSPNAYLRNPWNFIDFCVLISMWI
					S2 * S3
				Consensus sequence	.....F...F..E...K....G.....Y.R..WN..D..... F K. F H

FIGURE 2. **Multiple amino acid sequence alignment of the domain III S2--S3 linker of various VGCC α_1 subunits and candidates.** Multiple amino acid sequence alignment was performed with ClustalW (align.genome.jp). The completely conserved glycine residues, including the Cch1 Gly^{1265}, are colored *red* and highlighted by an *asterisk*, and the conserved acidic residues *green*. The putative S2 and S3 segments are *underlined* at the bottom. As for S3, a part of the amino acid sequence is shown. The full names of the species are (from the top to the bottom): *Homo sapiens*; *Oryctolagus cuniculus*; *Mus musculus*; *Rattus norvegicus*; *Gallus gallus*; *Danio rerio*; *Loligo bleekeri*; *Drosophila melanogaster*; *Caenorhabditis elegans*; *Neurospora crassa*; *Magnaporthe grisea*; *Aspergillus nidulans*; *Cryptococcus neoformans*; *Schizosaccharomyces pombe*; *Candida albicans*; *Ashbya gossypii*; and *S. cerevisiae*. Abbreviations: *1*, voltage-gated channel like; *2*, voltage-dependent calcium channel; *3*, cacophony; *4*, narrow abdomen; *5*, egg laying defective protein; *6*, uncoordinated protein; *7*, calcium channel α subunit; *8*, nematode calcium channel; *9*, voltage-gated ion channel.

We have confirmed, with Western blotting, that the amount of the mutant proteins was comparable with that of the wild-type Cch1 when they were produced from the self-promoter, and that it was at least 15-fold greater than that of the wild-type Cch1 when produced from the *TDH3* promoter (data not shown).

When the activities of the mutant proteins produced under the self-promoter were compared, the Gly-Ser and Gly-Ala substitutions reduced the Ca^{2+} uptake activity by ~30%, but did not affect cell viability (Fig. 4, *A* and *D*), indicating that the remaining ~70% Ca^{2+} uptake activity is sufficiently high to support the viability of cells. The Gly-Asp substitution slightly reduced both the cell viability and Ca^{2+} uptake activity. The Gly-Asn substitution inactivated the Ca^{2+} uptake activity, whereas it still maintained slight viability. Finally, the Gly-Thr, Gly-Val, Gly-Gln, Gly-Leu, and Gly-Lys substitutions resulted in the complete loss of Cch1 function. It is notable that when these mutant proteins were produced under the *TDH3* promoter, the viability and Ca^{2+} uptake activity were only slightly increased in the partially active mutant proteins and were not increased at all in the completely inactivated mutant proteins (Fig. 4, *A* and *D*), suggesting that a decrease in the amount of the mutant proteins is not a factor for the decrease in the viability and Ca^{2+} uptake activity.

When those results obtained with the self-promoter were re-plotted in terms of the residue volume or hydrophobicity of the amino acids, we noted a clear relationship between the residue volume and activity of the mutant proteins: Fig. 4, *B* and *E*, show that when the residue volume is ~115 cubic Å or greater at the position of Gly^{1265}, the Cch1 protein completely loses its activity. By contrast, Fig. 4, *C* and *F*, show that there is no relationship between hydrophobicity and Cch1 function. We therefore conclude that Gly^{1265} is important for Cch1 activity because of the smallest residue volume. Finally, we note that among the Gly-Asp, Gly-Asn, and Gly-Thr substitutions, three of which result in almost the same residue volume, the more the residue is

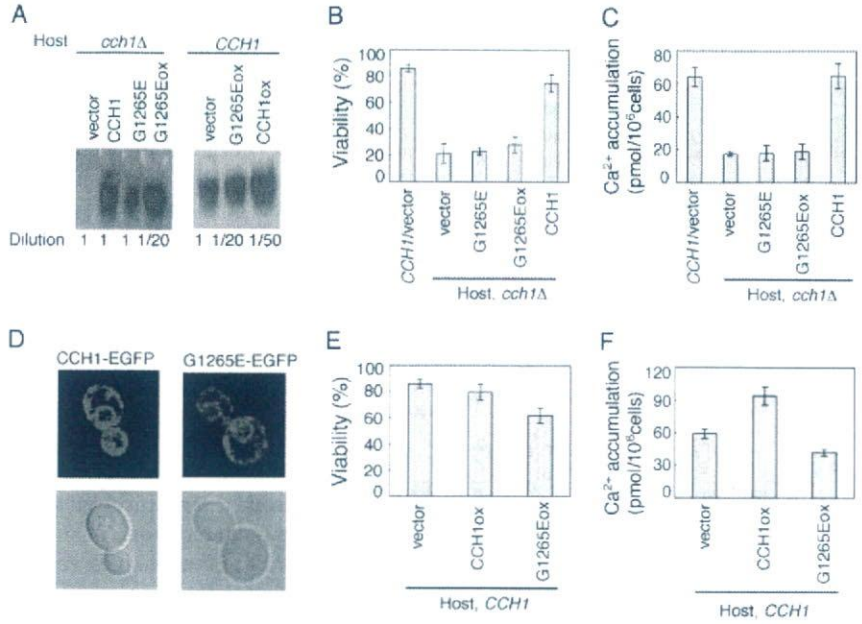

FIGURE 3. **Characterization of the *cch1-1* mutation.** *A*, Western blotting of the Cch1G1265E protein produced from the *cch1-1* gene on a plasmid. *Left panel*, the H317 strain (*cch1Δ*) was transformed with various plasmids and the extracts of the resulting transformants were subjected to Western blotting. Plasmids used here: *vector*, pBC111; *CCH1*, pBCS-CCH1H; *G1265E*, pBCS-CCH1Hm1; *G1265Eox*, pBCT-CCH1Hm1. *Right panel*, the parental strain H207 (*CCH1*) was transformed and treated as above. Plasmids used here: *vector*, pBC111; *G1265Eox*, pBCT-CCH1Hm1; *CCH1ox*, pBCT-CCH1H. Note that the samples were appropriately diluted as indicated *under* the panels. *B*, the viability of cells incubated with 6 μM α-factor for 8 h in SD.Ca100 medium. The transformants used here were the same as the *left panel* of *A*. *C*, Ca^{2+} accumulation of cells during a 2-h incubation with 6 μM α-factor in SD.Ca100 medium. The transformants used here were the same as in *B*. *D*, subcellular localization of Cch1G1265E-EGFP. Exponentially growing cells of *cch1Δ*/pBCT-CCH1H-EGFP (*left panels*) and *cch1Δ*/pBCT-CCH1Hm1-EGFP (*right panels*) in SD.Ca100 medium were observed by confocal fluorescence microscopy (*upper panels*) or differential interference contrast microscopy (*lower panels*). Essentially the same results were obtained for two additional experiments. *E*, viability of cells incubated with 6 μM α-factor for 8 h in SD.Ca100 medium. The transformants used here were the same as the *right panel* of *A*. Vector *versus* G1265E ($p < 0.05$). *F*, Ca^{2+} accumulation of cells during a 2-h incubation with 6 μM α-factor in SD.Ca100 medium. The transformants used were the same as those in *E*. Vector *versus* G1265E ($p < 0.05$). In *B*, *C*, *E*, and *F*, all the data are mean ± S.D. from at least three independent experiments.

brane in BHK6 cells (supplemental materials Fig. S1). However, some fraction appeared to remain in the cytoplasm. Almost all fractions of the rbCIIG959E, rbCIIG959K, and rbCIIG959A proteins were mainly present in the cytoplasm. By contrast, the rbCIIG959S protein was completely localized to the plasma membrane. These results indicate that the Gly-Ser substitution in rbCII results in marked attenuation of channel activity without altering the localization efficiency of the protein. The Gly-Glu, Gly-Lys, and Gly-Ala substitutions bring about a complete loss of channel activity, and this loss may be due to a decreased efficiency of protein transport to the plasma membrane.

DISCUSSION

Here we have shown the importance of the Gly residue present in the domain III S2–S3 linker of the yeast putative VGCC α_1 subunit Cch1 and of the rat VGCC α_1 subunit rbCII, a member of $Ca_v1.2$. Based upon a conventional transmembrane prediction (33), the domain III S2–S3 linker of VGCCs is composed of 13 amino acid residues and the Gly residue is the only one amino acid residue that is completely conserved in the linker (Fig. 2). This suggests that the Gly residue is indispensable for the function of VGCCs, and we have proven this suggestion.

Our study on the Cch1G1265E protein have indicated that Gly^{1265} is required for the function of Cch1, but probably not for the stability and subcellular localization of this protein because the amount of Cch1G1265E and the localization of Cch1G1265E-EGFP are essentially the same as those of the wild-type counterparts (Fig. 3, *A* and *D*). The reason for the importance of the Gly residue is that it has the smallest side chain, as revealed by systematic amino acid substitution experiments (Fig. 4).

As for rat rbCII, on the other hand, Gly^{959} may be important for not only function but also localization. The rbCIIG959E, rbCIIG959S, rbCIIG959K, and rbCIIG959A proteins have no or very little Ba^{2+} current, as revealed by patch clamp analysis. Indirect fluorescent immunomicroscopy has shown that, among these mutant proteins, the majority of the rbCIIG959E, rbCIIG959K, and rbCIIG959A proteins seem to be localized in the cytoplasm, instead of localization to the plasma membrane (supplemental materials Fig. S1). In addition, many of even the wild-type rbCII protein appears to remain in the cytoplasm. We speculate

hydrophilic, the higher the activity of the Cch1 product (Fig. 4, *C* and *F*).

Gly^{959} of Rat $Ca_v1.2$ Is Essential—On the basis of the above findings that the Gly^{1265} of Cch1 is essential and that the Gly residue positionally corresponding to Gly^{1265} is completely conserved during evolution, we examined the possibility that the Gly residue of mammalian VGCC α_1 subunits is essential for their channel function. To do this, the Gly^{959} residue of the rat $Ca_v1.2$ (rbCII), which is the positional counterpart of the Gly^{1265} of Cch1, was replaced with Glu, Ser, Lys, or Ala. The resulting mutant rbCII proteins were expressed under the control of the CMV promoter in BHK6 cells expressing rabbit β_{1a} and α_2/δ subunits and examined for their function and subcellular localization.

Whole cell patch clamp recordings showed that the rbCIIG959E protein had no channel activity at all and that the rbCIIG959S protein had little activity (Fig. 5). The rbCIIG959K and rbCIIG959A proteins had no activity at all (data not shown).

Confocal fluorescent microscopy with antibodies specific to rbCII showed that a significant fraction of the wild-type rbCII protein, used as a control, was localized to the plasma mem-

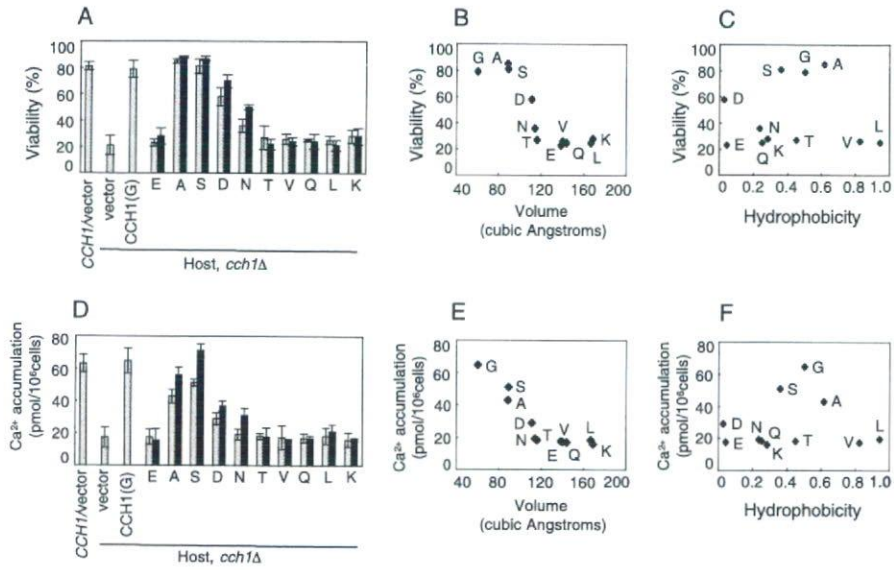

FIGURE 4. **Effect of the substitution of various amino acids for Gly^{1265} on Cch1 function.** Cells of the *cch1Δ* mutant expressing a Cch1 protein having a mutation in Gly^{1265} from the self-promoter or *TDH3* promoter were grown in SD.Ca100 medium, exposed to α-factor, and examined for viability and Ca^{2+} accumulation. *A*, the viability of cells was determined 8 h after exposure to α-factor. *Open* and *closed bars* represent the viability of cells expressing a mutant Cch1 protein produced from the self-promoter and the *TDH3* promoter, respectively. Mean ± S.D. from at least three independent experiments. Plasmids used: *vector*, pBC111; *CCH1 (G)*, pBCS-CCH1H; single letters from Glu to Lys represent the substituted amino acids at Gly^{1265}. Amino acid abbreviation: *G*, Gly; *E*, Glu; *A*, Ala; *S*, Ser; *D*, Asp; *N*, Asn; *T*, Thr; *V*, Val; *Q*, Gln; *L*, Leu; *K*, Lys. *B*, replot of the viability data shown in *A* as a function of the volume of amino acid residues (38). The data based on the self-promoter are shown. *C*, replot of the viability data shown in *A* as a function of the hydrophobicity of amino acid residues (39). The data based on the self-promoter are shown. *D*, Ca^{2+} accumulation was determined 2 h after the cells were exposed to α-factor. *Open* and *closed bars* represent the data obtained based on the self-promoter and the *TDH3* promoter, respectively. Mean ± S.D. from at least three independent experiments. Plasmids used and amino acid abbreviations were the same as those in *A*. *E*, replot of the Ca^{2+} accumulation data shown in *D* as a function of the volume of amino acid residues. The data based on the self-promoter are shown. *F*, replot of the Ca^{2+} accumulation data shown in *D* as a function of the hydrophobicity of amino acid residues. The data based on the self-promoter are shown.

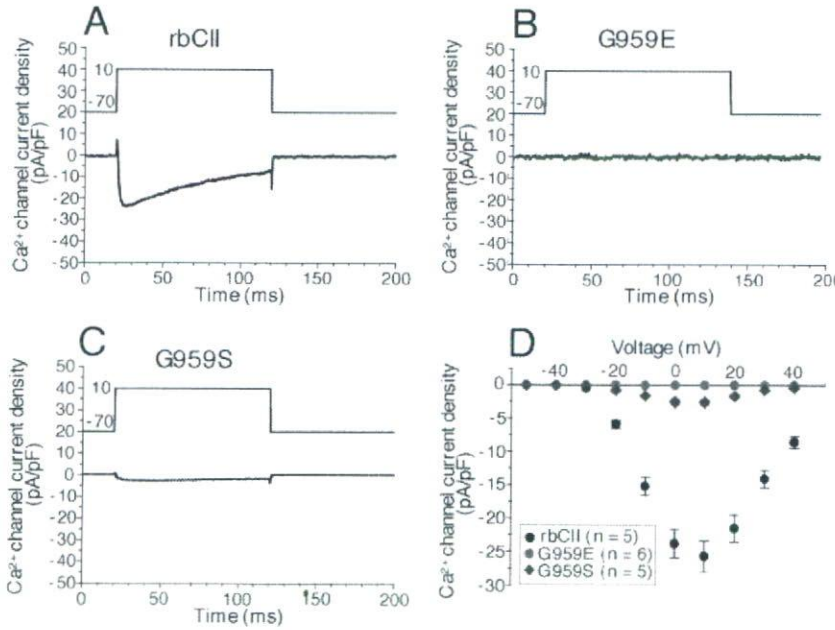

FIGURE 5. **Effects of substitution of various amino acids for Gly^{959} on the Ca^{2+} channel activity of rbCII.** Whole cell recordings of Ba^{2+} currents through the L-type Ca^{2+} channel rbCII and its mutant proteins expressed in BHK6 cells were shown. *A*, wild-type rbCII; *B*, the rbCIIG959E protein; *C*, the rbCIIG959S protein. The dysfunction of G959E could be due to the impairment of plasma membrane targeting (see supplemental materials Fig. S1). G959S showed markedly small Ba^{2+} currents, although it was localized to the plasma membrane (see supplemental Fig. S1). *D*, current-voltage relationships (I-V curve) of wild-type and mutant rbCIIs (G959E and G959S).

that overexpression of rbCII mRNA driven by the strong CMV promoter might have resulted in the mislocalization of these proteins because of excess in the amount of the α_1 subunit over that of the β and α_2/δ subunits. It is known that the correct targeting of the α_1 subunit to the plasma membrane requires the β subunit (23). By contrast, rbCIIG959S seems to be efficiently transported to the plasma membrane. Taken together, it is likely that Gly^{959} is necessary for the function and localization of rbCII.

From a structural viewpoint of voltage-gated ion channels, we speculate that the Gly residue has a role for the formation of a voltage-sensing structure composed of the S1–S4 segments. Among six transmembrane segments, the S1–S4 segments are considered to function as the voltage sensor of structurally related, voltage-gated Ca^{2+}, K^+, and Na^+ channels (2). In the case of K^+ channels whose structure is best elucidated, the four most extracellularly located basic residues of the S4 segment and the most intracellular acidic residue in the S2 segment are the major contributors to the gating charge movement that is coupled with the opening or closing of the pore of the channel (34, 35). In addition, according to the helix-packing model, the interaction of conserved negative charges in S2 and S3 with the conserved positive charges in S4 makes S2 and S3 line one side of the gating canal (36, 37). Thus, it is likely that the structure of the S2–S3 linker is also important for channel gating and the replacement of the Gly residue with any larger amino acid perturbs the spatial arrangement of S2 and S3. This perturbation may also affect the localization efficiency of VGCC α_1 subunits, as seen in rbCII.

Finally, we would like to point out that the Gly residue of the S2–S3 linker is present not only in domain III but also in domains I, II, and IV with a slight exception (data not

shown). Therefore, the Gly residue should have an essential function in all of the four domains.

Acknowledgments—We thank Dr. Chikara Sato for critical reading of the manuscript and fruitful discussion, Profs. Hiromichi Tsuru and Masahiro Sokabe for encouragement, and Yumiko Higashi for secretarial assistance.

REFERENCES

1. Berridge, M. J., Bootman, M. D., and Roderick, H. L. (2003) *Nat. Rev. Mol. Cell. Biol.* **4,** 517–529
2. Catterall, W. A. (2000) *Annu. Rev. Cell Dev. Biol.* **16,** 521–555
3. Lehmann-Horn, F., and Jurkat-Rott, K. (1999) *Physiol. Rev.* **79,** 1317–1372
4. Boycott, K. M., Maybaum, T. A., Naylor, M. J., Weleber, R. G., Robitaille, J., Miyake, Y., Bergen, A. A. B., Pierpont, M. E., Pearce, W. G., and Bech-Hansen, N. T. (2001) *Hum. Genet.* **108,** 91–97
5. Striessnig, J., Hoda, J.-C., Koschak, A., Zaghetto, F., Mullner, C., Sinnegger-Brauns, M. J., Wild, C., Watschinger, K., Trockenbacher, A., and Pelster, G. (2004) *Biochem. Biophys. Res. Commun.* **322,** 1341–1346
6. Mantuano, E., Veneziano, L., Spadaro, M., Giunti, P., Leggio, M. G., Verriello, L., Wood, N., Jodice, C., and Frontali, M. (2004) *J. Med. Genet.* **41,** e82
7. Guida, S., Trettel, F., Pagnutti, S., Mantuano, E., Tottene, A., Veneziano, L., Fellin, T., Spadaro, M., Stauderman, K., Williams, M., Volsen, S., Ophoff, R., Frants, R., Jodice, C., Frontali, M., and Pietrobon, D. (2001) *Am. J. Hum. Genet.* **68,** 759–764
8. Jen, J., Wan, J., Graves, M., Yu, H., Mock, A. F., Coulin, C. J., Kim, G., Yue, Q., Papazian, D. M., and Baloh, R. W. (2001) *Neurology* **57,** 1843–1848
9. Imbrici, P., Jaffe, S. L., Eunson, L. H., Davies, N. P., Herd, C., Robertson, R., Kullmann, D. M., and Hanna, M. G. (2004) *Brain* **127,** 2682–2692
10. Fischer, M., Schnell, N., Chattaway, J., Davies, P., Dixon, G., and Sanders, D. (1997) *FEBS Lett.* **419,** 259–262
11. Paidhungat, M., and Garrett, S. (1997) *Mol. Cell. Biol.* **17,** 6339–6347
12. Muller, M. E., Locke, E. G., and Cunningham, K. W. (2001) *Genetics* **159,** 1527–1538
13. Iida, K., Tada, T., and Iida, H. (2004) *FEBS Lett.* **576,** 291–296
14. Locke, E. G., Bonilla, M., Liang, L., Takita, Y., and Cunninghum, K. W. (2000) *Mol. Cell. Biol.* **20,** 6686–6694
15. Bonilla, M., Nastase, K. K., and Cunningham, K. W. (2002) *EMBO J.* **21,** 2343–2353
16. Matsumoto, T. K., Ellsmore, A. J., Cessna, S. G., Low, P. S., Pardo, J. M., Bressan, R. A., and Hasegawa, P. M. (2002) *J. Biol. Chem.* **277,** 33075–33080
17. Iida, H., Nakamura, H., Ono, T., Okumura, M. S., and Anraku, Y. (1994) *Mol. Cell. Biol.* **14,** 8259–8271
18. Kanzaki, M., Nagasawa, M., Kojima, I., Sato, C., Naruse, K., Sokabe, M., and Iida, H. (1999) *Science* **285,** 882–886
19. Kanzaki, M., Nagasawa, M., Kojima, I., Sato, C., Naruse, K., Sokabe, M., and Iida, H. (2000) *Science* **288,** 1347
20. Snutch, T. P., Tomlinson, W. J., Leonard, J. P., and Gilbert, M. M. (1991) *Neuron* **7,** 45–57
21. Tomlinson, W. J., Stea, A., Bourinet, E., Charnet, P., Nargeot, J., and Snutch, T. P. (1993) *Neuropharmacology* **32,** 1117–1126
22. Yamaguchi, S., Okumura, Y., Nagao, T., and Adachi-Akahane, S. (2000) *J. Biol. Chem.* **275,** 41504–41511
23. Gao, T., Chien, A. J., and Hosey, M. M. (1999) *J. Biol. Chem.* **274,** 2137–2144
24. Iida, H., Yagawa, Y., and Anraku, Y. (1990) *J. Biol. Chem.* **265,** 13391–13399
25. Sikorski, R. S., and Hieter, P. (1989) *Genetics* **122,** 19–27
26. McAlister, L., and Holland, M. J. (1982) *J. Biol. Chem.* **257,** 7181–7188
27. Jones, J. S., and Prakash, L. (1990) *Yeast* **6,** 363–366
28. Gietz, R. D., and Sugino, A. (1988) *Gene (Amst.)* **74,** 527–534
29. Chang, H.-C. J., Nathan, D. F., and Lindquist, S. (1997) *Mol. Cell. Biol.* **17,** 318–325
30. Higuchi, R., Krummel, B., and Saiki, R. K. (1988) *Nucleic Acids Res.* **16,** 7351–7367
31. Tada, T., Ohmori, M., and Iida, H. (2003) *J. Biol. Chem.* **278,** 9647–9654
32. Sherman, F., Fink, G. R., and Hicks, J. B. (1986) *Methods in Yeast Genetics,* Cold Spring Harbor Laboratory Press, Cold Spring Harbor, NY
33. Jan, L. Y., and Jan, Y. N. (1990) *Nature* **345,** 672
34. Aggarwal, S. K., and MacKinnon, R. (1996) *Neuron* **16,** 1169–1177
35. Seoh, S.-A., Sigg, D., Papazian, D. M., and Bezanilla, F. (1996) *Neuron* **16,** 1159–1167
36. Li-Smerin, Y., Hackos, D. H., and Swaritz, K. J. (2000) *J. Gen. Physiol.* **115,** 33–49
37. Cuello, L. G., Cortes, D. M., and Perozo, E. (2004) *Science* **306,** 491–495
38. Zamyatnin, A. A. (1972) *Prog. Biophys. Mol. Biol.* **24,** 107–123
39. Black, S. D., and Mould, D. R. (1991) *Anal. Biochem.* **193,** 72–82

ELSEVIER

Brain Research Bulletin 74 (2007) 376–384

BRAIN RESEARCH BULLETIN

www.elsevier.com/locate/brainresbull

Research report

Immunolocalization of muscarinic receptor subtypes in the reticular thalamic nucleus of rats

Satoko Oda [a,*], Fumi Sato [a], Akiko Okada [a], Satomi Akahane [b], Hiroaki Igarashi [a], Junko Yokofujita [a], Junli Yang [a], Masaru Kuroda [a]

[a] *Department of Anatomy, Toho University School of Medicine, Ota-ku, Tokyo 143-8540, Japan*
[b] *Department of Pharmacology, Toho University School of Medicine, Ota-ku, Tokyo 143-8540, Japan*

Received 9 November 2006; received in revised form 24 April 2007; accepted 5 July 2007
Available online 6 August 2007

Abstract

In this study, to identify the precise localization of the muscarinic receptor subtypes m2, m3 and m4 in the rostral part of the rat reticular thalamic nucleus (rRt), namely, the limbic sector, we used receptor-subtype-specific antibodies and characterized the immunolabeled structures by light, confocal laser scanning, and electron microscopies. The m2-immunolabeling was preferentially distributed in the distal dendrite region where cholinergic afferent fibers tend to terminate and in the peripheral region of somata, whereas the m3-immunolabeling was more preferentially distributed in a large part of somata and in proximal dendrite shafts than in the distal dendrite region. Dual-immunofluorescence experiments demonstrated that majority of rRt neurons with parvalbumin immunoreactivity contain both m2 and m3. Neither m2 nor m3 was detected in presynaptic terminals or axonal elements. No m4-immunolabeling was detected in the rostral part of the thalamus including rRt. These results show the different distributions of m2 and m3 in rRt neurons, and strongly suggest that m2 is more closely associated with cholinergic afferents than m3.

Keywords: Muscarinic receptor subtype; Immunocytochemistry; Reticular thalamic nucleus; Electron microscopy; Rat

1. Introduction

The thalamus is a strategic gating point where cholinergic innervations exert activation effects on the transmission of information from the subcortical regions toward target cortices. This cholinergic activation of the thalamocortical system is caused by two distinct cholinergic mechanisms [34,54]. In one mechanism, acetylcholine directly causes a slow and long-lasting depolarization of thalamic relay neurons and the transition of their neuronal firing mode from a rhythmic burst mode to a single spike mode [11,31,59]. In the other mechanism, acetylcholine causes the hyperpolarization of two major GABAergic inhibitory elements, i.e., reticular thalamic nucleus (Rt) neurons and interneurons, and the transition of their neuronal firing mode to a rhythmic burst mode [24,32,33]. Furthermore, the rate of γ-aminobutyric acid (GABA) release from inhibitory neurons decreases with the application of muscarinic agonists [47]. As a result of the latter mechanism, the GABAergic inhibition of relay neurons is suppressed. For this reason, the latter is the so-called disinhibition mechanism. Because both cholinergic mechanisms depend on muscarinic acetylcholine receptors, the type of muscarinic receptor that is predominantly active must differ between the mechanisms.

Muscarinic acetylcholine receptors have been classified into five subtypes, that is, m1–m5, according to the sequences of the genes encoding them. Biochemical studies have revealed that m1, m3 and m5 preferentially couple to stimulate phospholipase C activity, whereas m2 and m4 couple to inhibit adenylcyclase activity [7]. Additionally, electrophysiological studies have shown that m1 and m3 are associated with the inhibition of M-current, that is, the activation of these receptors may block the adaptation of neurons, whereas m2 and m4 are associated with the activation of potassium channels [22,46]. A previous study revealed the different localizations of muscarinic receptor subtypes in the relay neurons of the anteroventral thalamic nucleus (AV) that receive dense cholin-

* Corresponding author. Tel.: +81 3 3762 4151x2323; fax: +81 3 5493 5437.
E-mail address: odas@med.toho-u.ac.jp (S. Oda).

0361-9230/$ – see front matter © 2007 Elsevier Inc. All rights reserved.
doi:10.1016/j.brainresbull.2007.07.017